NON-DESTRUCTIVE EVALUATION METHOD BASED ON DYNAMIC INVARIANT STRESS RESULTANTS

A Thesis

by

JUNCHI ZHANG

Submitted to the Office of Graduate and Professional Studies of
Texas A&M University
in partial fulfillment of the requirements for the degree of

MASTER OF SCIENCE

Chair of Committee,	Luciana R. Barroso
Committee Members,	Stefan Hurlebaus
	Fanis Strouboulis
Head of Department,	Robin Autenrieth

May, 2015

Major Subject: Civil Engineering

ABSTRACT

During the past five decades, research in damage detection has been rapidly expanding. Most of the methods explored are based on changes in frequencies, mode shapes, mode shape curvature, and flexibilities. These methods can only detect and locate damage. Current methods can seldom identify the exact severity of damage to structures. In this research, a new non-destructive evaluation method is proposed to identify the existence, location, and severity of damage for structural systems. Additionally, damage in mass, damping and stiffness will be characterized. The goal of this research is to develop the concept of Dynamic ISR method and apply it to specific types of structures. The method utilizes dynamic analysis of the structures to simulate direct measurements of acceleration, velocity and displacement simultaneously. Numerical results demonstrate that the application of the method will reflect the advanced sensitivity and accuracy of the method in characterizing multiple damage locations.

DEDICATION

I dedicate this thesis to my family, especially to my father and mother.

ACKNOWLEDGEMENTS

It is a great pleasure to make this thesis possible.

I am heartily thankful to my committee chair, Dr. Lucinana R. Barroso, for her encouragement, supervision and support throughout the research. She gives me the opportunity to continue my research when I am confused about my future. Moreover, her advice always helps me to focus on the core of the research. Also, I would like to express the deepest appreciation to my committee member Dr. Stefan Hurlebaus. His enthusiasm for the research and attitude towards difficulties inspired me a lot. Without his guidance and persistent help, this defense would not be possible. I would also like to thank Dr. Fanis Strouboulis, not only for his help and support throughout the research but also for his finite element class which helps me to use FEM to solve problems.

I also would like to specially thank Dr. Norris Stubbs, for his spirit and talent. It is his patient guidance that gives me the general idea of the research direction.

And I would like to thank my dear friend, Ran Li, who helped me a lot during the whole process of the research.

Thanks also go to my friends and colleagues and the department faculty and staff for making my time at Texas A&M University a great experience.

Finally, thanks to my mother and father for their continual encouragement.

NOMENCLATURE

ISR	Invariant Stress Resultants
NDE	Non-destructive Evaluation
SHM	Structural Health Monitoring
DOF	Degree of Freedom
SDOF	Single Degree of Freedom
2-DOF	Two Degree of Freedom
5-DOF	Five Degree of Freedom
MDOF	Multi-Degree of Freedom
FEA	Finite Element Analysis
MAC	Modal Assurance Criterion
COMAC	Coordinate Modal Assurance Criterion
STRECH	Structural Translational and Rotational Error Checking

TABLE OF CONTENTS

LIST OF FIGURES

LIST OF TABLES

CHAPTER I

INTRODUCTION

1.1 Overview

Damage is the main cause of structural failures. In order to avoid failure, it is important to identify the minor damage early on. Damage can appear as cracks, corrosion and spalling, as well as local deformation both inside and outside the structures. Yao (1972) gave a definition of damage as "the occurrence of any modification in a part, or parts of a structure that can impair the intended performance of the structure." From this definition, damage identification must compare two different states of structures. One is initial state, or undamaged state. The second is the final state (Farrar and Worden, 2007). Therefore, the definition of damage provides a general idea on how to obtain the current performance changes of a system, such as material and geometric properties. Figure I.1depicts a structure with cracks, corrosion / spalling and deformation.

Figure I.1 Concept of damage (Federal Highway Administration, 2007)

In a general case, compliance, mass, damping and stiffness of the i^{th} member of the system can be defined as F_i, m_i, c_i and k_i, with changes defined as δF_i, δm_i, δc_i and δk_i respectively. Local mechanical manifestations of damage can be described as:

- Increase in compliance (crack): $\delta F_i > 0$
- Decrease in stiffness (crack, corrosion): $\delta k_i < 0$
- Increase in damping (closed crack): $\delta c_i > 0$
- Decrease in damping (open crack): $\delta c_i < 0$
- Increase in mass (flooding): $\delta m_i > 0$
- Decrease in mass (corrosion): $\delta m_i < 0$

Knowing the mechanical manifestation of damage is not enough. Our research goal is to identify and predict damage so as to decrease loss. Structural Health Monitoring (SHM) involves the process of implementing a damage identification and an evaluation of the current status of the system health. In the long-term, because of the operational environment, the inevitable aging and damage accumulation will impact the intended performance of the structure. The output of SHM process periodically renews the information, which shows the current state of the structure. Under the external events, such as an earthquake or wind loads, SHM provides rapid condition screening to display the reliable information about system states and operational evaluation of the system (Farrar and Worden, 2007).

Rytter (1993) gives the four principal damage stages of structural health monitoring:

- Level I: Only identify if damage has occurred
- Level II: Identify and locate damage
- Level III: Identify, locate and estimate the severity of damage
- Level IV: Identify, locate, estimate, and evaluate the impact of damage on the structure.

Non-destructive evaluation (NDE) is a wide set of analysis approaches used to perform SHM without causing damage to the physical structure. Thus, the above levels also can be used as a classification of NDE. The recently published methods mostly belong to the first two Levels. Level III & IV methods are what researchers work towards. The most generalized indicators to characterize the damage in a Level III NDE method can be explained in following equations (Stubbs, 1992):

$$Mass\ damage\ severity = \frac{\delta m_i}{m_i} \tag{1.1}$$

$$Damping\ damage\ severity = \frac{\delta c_i}{c_i} \tag{1.2}$$

$$Stiffness\ damage\ severity = \frac{\delta k_i}{k_i} \tag{1.3}$$

If the damage severity for a localized region equals to zero, there is no damage. Otherwise, damage is present in that region.

1.2 Objectives

The goal of this research is to propose an effective method to detect the existence, location and severity of damage to predict the state of the structures. The proposed dynamic ISR (Invariant Stress Resultants) method is developed and utilized to

detect the damage of corresponding changes in mass and stiffness in 1-D and 2-D models. The objectives of this research are to:

1) Develop the basic theory of dynamic ISR method and apply it to the specific types of structures.
2) Verify the accuracy of the developed theory using exact structural response quantities simulated from the static analysis of Finite Element models.

1.3 Significance

The proposed new method, dynamic ISR, is a Level III evaluation method that has the following advantages:

- The potential to provide a clear indicator of damage location.
- Potentially sensitive to small levels of damage and damage that occurs in inaccessible locations.
- Only experimental data, including acceleration, velocity and displacement is needed to complete the analyses. The values of external force, mass, stiffness, and damping do not need to be provided.
- Applicable to nearly all type of structure and multiple damage locations cases. It will detect mass, damping and stiffness change at the same time.
- May provide accurate quantitative values of mass, damping, and stiffness damage severities.
- Computational process is straight-forward and robust.

According to the advantages listed above, this theory has the potential to be a valuable Level III non-destructive evaluation method. If it can be widely used in the

field, it will help to evaluate service life of structures and deduct the loss caused by damages.

1.4 Limitations

Although the proposed dynamic ISR shows great significant performance in identification damage, it still incomplete to some extent. Some noted limitations include:

- The research mainly focuses on 1-D and 2-D structures. 3-D structures, such as plate structures, are not considered.
- For beam system, truss system and frame system, only mass and stiffness will be explained in detail, but damping damage is not considered.
- In practical situations, in order to get the exact location and severity of the damage, it may require data from closely-spaced sensors.

As a new member of NDE methods are available, additional research will be required to refine the dynamic ISR method address the above limitations.

CHAPTER II

BACKGROUND

Early development in vibration-based damage detection was performed in the late 1970s and early 1980s. Most proposed techniques were in the offshore oil industry (Vandiver, 1975, 1977; Wojnarowski et al., 1977; Whittome and Dodds, 1983). Because the waterline measurements can only provide information about resonant frequencies, the influence of the environmental conditions was not considered in the results. Thus, the oil industry almost abandoned pursuit of this methodology in the mid-1980s.

2.1 Current Methods

In the past three decades, methods of damage identification has become very broad for both local and global. In this paper, the literature review mainly focuses on the development of vibration-based damage detection.

2.1.1 Frequency Changes / Frequency-Change Ratios

Doebling (1996) and Salawu (1997) reviewed on the application of modal frequency changes for damage diagnostics. From these thorough reviews, researchers noticed that the shifts of frequency had significant practical limitations when applied to structures, although ongoing further work might help resolve these difficulties.

2.1.1.1 Level I Methods

Adams et al. (1978) used the change of frequency to classify glass fiber reinforced plastics and the cracks in unidirectional carbon. They used axial modes to identify and locate the damage in a one-dimensioned system. Cawley and Adams (1979)

provided a formulation to predict damage in composite materials based on the change of frequency. For each potential damaged location, they compared a number of mode shapes and overlapped the results to reduce the error to detect the damage. The drawback of this method is that it is not sensitive enough to identify multiple-damage locations.

Friswell et al. (1994) used an existing model of a structure to compute frequency changes of the first several modes for both the initial and the final states. Furthermore, they calculated the ratios of all the changes in frequency and compared the results. Two measures of fit were used: a correlation coefficient, and how close the exponent and coefficient are to unity. The quality of the fit to a known pattern of damage was the possibility of damage. Juneja, et al. (1997) proposed a new method called contrast maximization and provided a predictive measurement to detect damage. In this method, a database of responses was developed. By matching the different response data, damage in the structures could be detected.

2.1.1.2 Level II Methods

On the basis of the work of Cawley and Adams (1979), Stubbs and Osegueda (1990) developed an explicit damage identification technique using the sensitivity of modal frequency changes. In this method, only one damage location is assumed. An error function for each mode and each member is proposed as part of the method. The member, whose function has the minimum error value is defined as the damaged element. However, this method limited in that it relies on the sensitivity matrices based on the accuracy of the Finite Element Model (FEM). To solve this problem, Stubbs et al. (1992) developed the damage index method using mode shape curvature changes.

2.1.2 Mode Shape Changes

Allemang and Brown (1982) presented a new method, modal assurance criterion (MAC), to find the relationship between two groups of mode shapes. West (1984) used the same technique to determine the level of correlation between two modes. One of the modes is from the test of an undamaged Space Shuttle Orbiter body flap while the other mode is from the test of the flap after it had been exposed to acoustic loading. Lieven and Ewins (1988) presented the Co-ordinate Modal Assurance Criterion (COMAC) and used it as a damage detection index. MAC indicates the correlation between two sets of mode shapes. COMAC shows the correlation between the mode shapes at a selected measurement point of a structure.

Mayes (1992) presented a method called Structural Translational and Rotational Error Checking (STRECH), which accessed the precise of the different stiffness between two degrees of freedom by approaching model error localization. Ratcliffe (1997) proposed a technique focusing on beam-like structures, which using a Laplacian operator on mode shape data to do finite difference approximation. Cobb and Liebst (1997) did an eigenvector sensitivity analysis to present a method for prioritizing sensor locations for damage identification. Skjaeraek et al. (1996b) examined the optimal sensor location issue to do damage detection. By using a substructure iteration method, the changes in mode shapes and modal frequencies were computed.

2.1.3 Mode-Shape-Curvature / Strain Mode Shape Changes

2.1.3.1 Local changes in mode shape curvature

Pandey et al. (1991) introduced a new parameter called "mode shape curvature". By comparing the difference in the mode shape curvature between the initial and the final case, the crack of the FEM beam structure was located. By using the central difference operator, the values of mode shape curvature were calculated from the displacement mode shape.

2.1.3.2 Conservation of local fractional modal strain energy

Stubbs et al. (1992) presented a method called the damage index method, which relied on the decrease in modal strain energy in 2-DOF. The changes of the modal strain energy can be defined as the curvature of measured mode shapes. The basic assumption of this method is that the fractional strain energy of the j^{th} element is the same in both intact and damaged system.

Some researchers computed mode shape curvature from the acceleration and displacement while other researchers measured the strain directly. Chance et al. (1994) was one such researcher that used the measured strain instead of the measure curvature. This approach significantly avoids the unacceptable errors resulting from computing the mode shape curvature from acceleration and displacement data.

2.1.4 Increase in Flexibility

2.1.4.1 Flexibility Changes

Aktan et al. (1994) presented a method that used measured flexibility as a condition index to detect the relative integrity of two bridges. The presented complete

nodal system allows for strain-based measurement as well as testing and multi-input / multi-output forced excitation frequency response measurement. The results of the research demonstrated the reliable and feasible assessment to highway bridges. Toksoy and Aktan (1994) proposed a new technique that could indicate damage even without a baseline data set by observing the anomalies in the deflection profile. Zhang and Aktan (1995) suggested that changes in curvatures of the uniform load surface, which could also be the deformed shape of the structure when applied to a uniform load, are calculated from the experiment and analysis. They proposed that changes in the uniform load surface will be used as the indices as for measurement of structural analysis. This technique was applied to a highway bridge and the results showed very accurate damage indices.

Pandey and Biswas (1994, 1995) presented a Level II method based on curvature mode shape of structures. The curvature mode was shape computed from the displacement by using a central difference approximation. This method was applied to a cantilever beam and a simply supported analytical beam. Numerical examples showed that the first two measured modes of the structure could be used to obtain to realize the damage conditions and locations with the beam.

Mayes (1995) used measured flexibility to do damage detection on a bridge based on the results of a modal test. He also used measured flexibility as the input for a damage identification method (STRECH). By taking ratios of modal displacements, the presented method evaluated changes in the FEM. Peterson et al. (1995) developed a method to decompose flexibility matrix into elemental stiffness parameters for a known

structural connectivity. The process of decomposition was accomplished by projecting the flexibility matrix onto the element-level structural eigenvectors.

Catbas et al. (2008) developed a new method that is based on the changes in mode flexibility and flexibility curvature. They detected the existence of the damage by comparing flexibility-based displacement and curvature between the original and damaged structures. This new technique was demonstrated be very sensitive in the presence of damage in the system.

2.1.4.2 Effects of Residual Flexibility

The residual flexibility matrix indicated the contribution from modes outside the measured bandwidth so that the exact flexibility matrix could be associated with the measured modes and the residual flexibility. Doebling et al. (1996) presented a technique to estimate the residual flexibility between non-excited structural degrees of freedom from experimental vibration data. The technique completed the reciprocity of the residual flexible matrix. The result of the work demonstrated that the use of the rank-deficient flexibility should improve the result of the damage evaluation.

2.1.5 Invariant Stress Resultants Method

Dincal and Stubbs (2013) presented the Static Invariant Stress Resultants (ISR) method, which could accurately locate and size damage in a Timoshenko beam. Li and Stubbs (2013) expanded this method by using structural member energy strains to get the stiffness damage severity. The basic concept of invariant stress resultants is that at any given cross section the resultant internal force distribution in a structural member was not affected by the inflicted damage. The principal of the ISR method was that the local

damage decreases showed in the bending and shear stiffness in the structural member. These changes finally led to the variable of deformation properties generated from the static analysis. In order to accomplish the condition for the invariant stress resultants, the same static external forces were applied to the pre-damage and post-damage systems. Based on the invariant stress resultants, the ratio of pre-damage and post-damage elements strain energies equaled the ratio of stiffness. This method effectively avoids the consideration of the changes in mass and damping when detecting stiffness damage. The method was applied to 1-D, 2-D, and 3-D structures with single or multiple damage locations. This method shows very effective results in stiffness damage detection of structures during static loadings situations.

2.2 Limitations of Current Methods

2.2.1 Frequency Changes

In early publications, the proposed frequency change based methods fall into Level I damage identification, and most methods were used extensively by offshore oil industry investigators. The limitation posed by environmental conditions keeps the frequency shifts from precisely detecting damage. In more recent publications, some related methods had been developed that can be defined as Level II or Level III. However, these methods still show two main drawbacks: the limited range of damage scenarios and the low sensitivity of the frequencies to damages.

Additionally, modal frequencies, as a global property of the structure, generally cannot give spatial information about structural changes. The methods to overcome the limitation require higher modal frequencies, where the modes are related to local

responses. However, the local models, which are a part of the high modal density, are difficult to extract. Multiple changes of frequency can provide local information about structural damage for different combinations of modal frequencies shifts. However, it is difficult to get sufficient number of frequencies shifts to estimate the damage location uniquely.

2.2.2 Mode Shapes Changes

As mentioned preciously, the aim of SHM is to use damaged-sensitive features to determine the current states of the structures. However, the major drawback of MAC and COMAC is that neither are sensitive enough to realize small damages occurred in the early stages. The drawback of both of MAC and COMAC comes from the specific algorithms that distribute the differences resulting from the damage to all the measurement points (MAC) or to all the mode shapes (COMAC) (Heylen and Janter, 1989; Pandey et al., 1991).

2.2.3 Change of Mode Shape Curvature

Compared to the early methods, methods based on mode shape curvature are more sensitive. However, the major limitation is that it shows irreducible imprecision in detecting damage locations. When higher modes are utilized, false damaged locations will be detected. The false results will not disappear when refine system elements.

2.2.4 Changes of Flexibility

Pandey and Biswas (1994) presented the technique based on the flexibility matrix of the structures. Although this new method requires few lower frequency modes, they did not present a clear measurable index for damage. Also, it is a problem to obtain the

ortho-normalized modes when applying to modes obtained from ambient data (Farrar and Jauregui, 1996). On the basis of previous work, Catbas et al. (2008) developed a damage detection method based on flexibility and flexibility based curvature. This method only meets the requirement of Level I, detecting the existence of damage, but is invalid to determine the location and the estimation of damage severity.

2.2.5 Invariant Stress Resultants Method

Although the ISR method has produced effective results in identifying damage related to stiffness changes for specific structures, current approach assumes the external loads on the system are static. In many civil structural systems, the significant external forces arise from occupancy and usage of the structure, such as live loads, and from natural hazardous loads, such as earthquake and wind. These forces cannot be assumed to be static force under a performance analysis. On the other hand, the neglected mass and damping changes will apparently result in the changes of structures' service life

CHAPTER III

SINGLE DEGREE OF FREEDOM

3.1 Overview of dynamic ISR Method

As presented in 2.1.5, invariant stress resultant (ISR) means that the stress resultants are not affected by damage at any given cross section of a structural member. The ISR that is represented in local coordinates equals the external forces represented in global coordinates. Therefore, dynamic ISR method mainly focuses on establishing equations for invariant external forces compared to the existing static ISR method, which uses strain energies for a structural member. A benefit seen from this approach is that it is more straightforward and easy to implement, lending itself to computational efficiencies. Additionally, the values of the external force, the system mass, stiffness, and damping is not necessary during simulation.

The dynamic-ISR methodology assumes that the initial system and the final system are subjected to the same external loading. It also assumes that the connectivity between members remains constant in both pre-damage and post-damage cases. Furthermore, the new methodology comes from the fundamental principles of mechanics of certain structures undergoing vibration. For a mass-spring-damping system, the equation of motion of the simple structures has been used. Based on the data at a specific location, which contains acceleration, velocity, and displacement, basic equilibrium is used and the damage severity is solved by numerical method. Based on the results of the specific element, the existence, location, and severity of the damage can be detected.

3.2 Application to SDOF System

What follows is the description for a single degree of freedom (SDOF) mass-damping-spring system (Figure III.1). The mass, damping and stiffness for the pre-damaged system are m, c, and k and for the post-damaged system, are m^*, c^*, and k^*. The stress resultants for the pre-damage system and post-damage system both are $p(t)$. Based on the assumption of invariant stress resultants, the external dynamic forces for both cases are the same, $P(t)$.

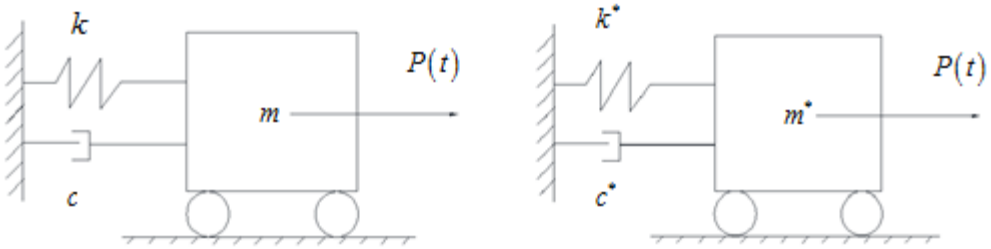

Figure III.1 Pre-damaged and post-damaged system for single degree of freedom

The equation of motion for the undamaged system is

$$m\ddot{x} + c\dot{x} + kx = P(t), \tag{3.1}$$

while the equation of motion for the damaged system is

$$m^*\ddot{x}^* + c^*\dot{x}^* + k^*x^* = P(t) \tag{3.2}$$

It is assumed that the initial acceleration $\ddot{x}$, velocity $\dot{x}$, displacement x and damaged acceleration $\ddot{x}^*$, velocity $\dot{x}^*$, displacement x^* are known at a specific time.

Because $P(t)$ is a function of time, the acceleration, velocity and displacement for both cases are functions of time.

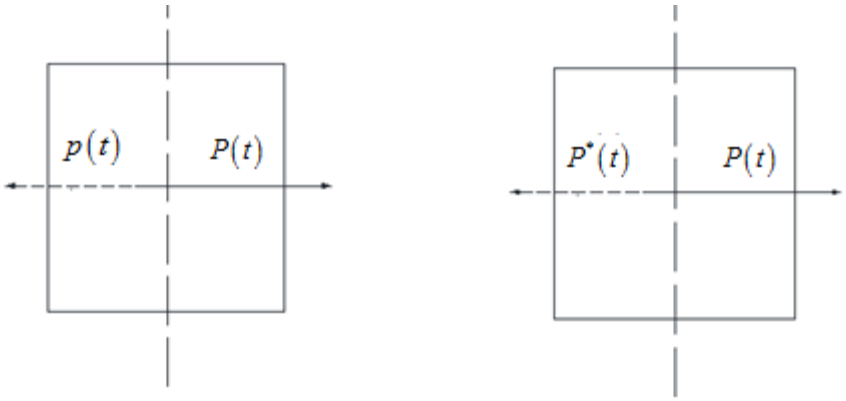

Figure III.2 Stress resultants and external force in initial and final system

In this example, the potential damage is expressed as a local decrease in mass, damping and stiffness in the structural member. At the cross-section, the consequence of the stress resultants shows the external force in the global coordinates (Figure III.2). As mentioned in the assumption, the external loading in both pre-damage and post-damage are the same. Based on this relationship, equations in global coordinates can be established to show the results of invariant stress resultants in local coordinates.

By equating Eq. (3.1) and Eq. (3.2),

$$m\ddot{x} + c\dot{x} + kx = m^*\ddot{x}^* + c^*\dot{x}^* + k^*x^* \tag{3.3}$$

$$\frac{m}{k^*}\ddot{x} - \frac{m^*}{k^*}\ddot{x}^* + \frac{c}{k^*}\dot{x} - \frac{c^*}{k^*}\dot{x}^* + \frac{k}{k^*}x = x^* \tag{3.4}$$

Assuming $t = t_1$, Eq. (3.4) can be written as

$$\begin{bmatrix} \ddot{x}(t_1) & -\ddot{x}^*(t_1) & \dot{x}(t_1) & -\dot{x}^*(t_1) & x(t_1) \end{bmatrix} \begin{bmatrix} \frac{m}{k^*} \\ \frac{m^*}{k^*} \\ \frac{c}{k^*} \\ \frac{c^*}{k^*} \\ \frac{k}{k^*} \end{bmatrix} = \begin{bmatrix} x^*(t_1) \end{bmatrix} \tag{3.5}$$

By solving Eq. (3.5), a new variable β_i can be defined as $\beta_1 = \frac{m}{k^*}$, $\beta_2 = \frac{m^*}{k^*}$, $\beta_3 = \frac{c}{k^*}$, $\beta_4 = \frac{c^*}{k^*}$, $\beta_5 = \frac{k}{k^*}$.

$$\beta_m = \frac{\beta_1}{\beta_2} = \frac{\left(\frac{m}{k^*}\right)}{\left(\frac{m^*}{k^*}\right)} \tag{3.6}$$

$$\beta_c = \frac{\beta_3}{\beta_4} = \frac{\left(\frac{c}{k^*}\right)}{\left(\frac{c^*}{k^*}\right)} \tag{3.7}$$

$$\beta_k = \beta_5 = \frac{k}{k^*} \tag{3.8}$$

The damage severity for mass, damping and stiffness are α_m, α_c ,. α_k

$$\alpha_m = \frac{1}{\beta_m} - 1 \tag{3.9}$$

$$\alpha_C = \frac{1}{\beta_c} - 1 \tag{3.10}$$

$$\alpha_k = \frac{1}{\beta_k} - 1 \tag{3.11}$$

Using the linear square method for several groups of equations, Eq. (3.5) written at different times, to solve for damage indicators will decrease errors.

3.3 Simulation Procedure for SDOF System,

In order to verify the presented theory, a mass-damping-spring model was built using SAP2000. The pre-damage model contains a particle and a link support, which can be taken as damping and stiffness. By decreasing the values of the mass of the particle and the coefficient of the link, a post-damage model can be developed. Then the same dynamic load, $P(t)$ was applied to the particle for both initial and final cases.

Table III.1 Damage parameters for seven damage cases

	Mass (kip-s^2)/in	Damping (kip-s/in)	Stiffness (kip/in)	Force Amplitude (kips)
Initial	3.00	1.00	2.00	1.00
Case 1	2.40	1.00	2.00	1.00
Case 2	3.00	0.90	2.00	1.00
Case 3	3.00	1.00	1.40	1.00
Case 4	2.40	0.90	2.00	1.00
Case 5	2.40	1.00	1.40	1.00
Case 6	3.00	0.90	1.40	1.00
Case 7	2.40	0.90	1.40	1.00

Table III.2 Actual Results for seven cases

Description of cases	Mass		Damping		Stiffness	
	β_m	α_m	β_c	α_c	β_k	α_k
Case 1 – Reduction in mass	1.25	-0.20	1.00	0.00	1.00	0.00
Case 2 – Reduction in damping	1.00	0.00	1.11	-0.10	1.00	0.00
Case 3 – Reduction in stiffness	1.00	0.00	1.00	0.00	1.43	-0.30
Case 4 – Reduction in mass and damping	1.25	-0.20	1.11	-0.10	1.00	0.00
Case 5 – Reduction in mass and stiffness	1.25	-0.20	1.00	0.00	1.43	-0.30
Case 6 – Reduction in damping and stiffness	1.00	0.00	1.11	-0.10	1.43	-0.30
Case 7 – Reduction in mass, damping and stiffness	1.25	-0.20	1.11	-0.10	1.43	-0.30

For the SDOF system, only one damage location can be applied, but multiple types of damages can be combined in the simulation cases. These different types of damages include reduction of the mass, damping, and stiffness. Seven different combinations were designed and can be summarized in Table III.1.

The acceleration, velocity and displacement for the initial and final system can be calculated directly by dynamic analysis using SAP2000. Using the data from the finite

element program, the damage indices and damage severity can be calculated. The actual values for damage indices and damage severity for each case are listed in Table III.2.

3.4 Results for SDOF System

Using the acceleration, velocity and displacement data from the pre-damage and post-damage systems, the damage indices and damage severity in every case can be calculated, which are listed in the Table III.3 and Table III.4. In Table III.3, the column of percent error shows the difference between the actual damage indices values and the calculated damage indices values. Similarly, in Table III.4, the absolute error provides the slight difference between the damage severities in initial and final systems. The reason to use absolute value for Table III.4 is to prevent zero as dominator when there is no changes in the parameters.

The damage indices showed in Table III.3 can reflect the ratio of the original parameters and post-damaged parameters. For example, when $\beta_m = 1.25$, it demonstrates the ratio of the initial mass to the final mass which equals 1.25. The percent error in Table III.3 indicates the error of initial and final damage indices over the initial one. And in all cases, the percent values are smaller than standard criterion, 2%. The results listed in Table III.4 can directly indicate the current state of the structures. For example, $\alpha_m = -0.20$, means a reduction in mass of 20%. The absolute error in Table III.4 expresses the absolute difference between the calculated damage severities and the actual one and the values are less than 0.02, which are very small. Compared results of the two tables, it clearly shows that Case 1, Case 2 and Case 3 reflect the reduction of single parameter cases, while Case 4, Case 5, Case 6 and Case 7 show the

changes in the multiple parameters cases. The results of Case 1 indicates the reduction of mass is 20%. The calculated values of indicator and damage severity show the changes in damping is 10%. Case 3 provides the results for the value decrease in stiffness is 30%. Case 4 is the combination of Case 1 and Case 2. Case 5 shows the equivalent results of the combination of Case 1 and Case 3. For Case 6, the results show the damage reduction cases as the combination of Case 2 and Case 3. As for Case 7, the calculated indicators and severities show that the reduction of mass, damping and stiffness are 20%, 10% and 30%.

Table III.3 Calculated damage indices for seven cases

Damage Case	$\beta_m = m / m^*$		$\beta_c = c / c^*$		$\beta_k = k / k^*$	
	Calc. Value	Percent Error	Calc. Value	Percent Error	Calc. Value	Percent Error
Case 1	1.25	-1.32E-08	1.00	5.93E-06	1.00	-3.10E-06
Case 2	1.00	-1.40E-08	1.11	-1.00E-03	1.00	-2.7E-06
Case 3	1.00	-7.6E-09	1.00	9.3E-08	1.43	-1.00E-04
Case 4	1.25	-1.5E-08	1.11	-1.00E-02	1.00	-3.00E-06
Case 5	1.25	-2.00E-08	1.00	2.45E-06	1.43	-1.00E-04
Case 6	1.00	-2.00E-08	1.11	-1.00E-02	1.00	-1.10E-04
Case 7	1.25	-4.97E-09	1.11	-1.00E-03	1.43	-6.10E-06

Notes: (1) Number of the time step for each case is 50
(2) The output time step size 0.05

Table III.4 Calculated damage severity for seven damage cases

Damage Case	$\alpha_m = 1/\beta_m - 1$		$\alpha_c = 1/\beta_c - 1$		$\alpha_k = 1/\beta_k - 1$	
	Calc. Value	Absolute Error	Calc. Value	Absolute Error	Calc. Value	Absolute Error
Case 1	-0.20	1.06E-10	0.00	5.93E-08	0.00	3.07E-08
Case 2	0.00	1.43E-10	-0.10	8.9E-05	0.00	2.70E-08
Case 3	0.00	7.62E-11	0.00	9.30E-10	-0.30	7.19E-07
Case 4	-0.20	1.17E-10	-0.10	9.00E-05	0.00	2.97E-08
Case 5	-0.20	1.61E-10	0.00	2.45E-08	-0.30	7.45E-07
Case 6	0.00	1.55E-10	-0.10	9.00E-05	-0.30	7.49E-07
Case 7	-0.20	3.97E-11	-0.10	-9.00E-06	-0.30	4.30E-08

Notes: (1) Number of the time step for each case is 50
(2) The Output time step size 0.05

3.5 Conclusions for SDOF System

By comparing the results from different cases, the following conclusions can be drawn effectively,

- The application of dynamic ISR method in SDOF indicates the superiority of a Level III method. Although the SDOF model repeatedly simulated one damage location, it still provided very effective results to identify the type and the severity of the damage. Some damage index errors can be very small. All of the results are less than the standard detection error, 2%.

- Based on the calculated damage indices, it is easy to qualify the damage severity, which is contributed to learning the exact state of the structure.
- Dynamic ISR method can detect the changes in the mass, stiffness and damping without knowing any of the system parameters.
- Detection by dynamic ISR method in a SDOF system is not limited to structures with one damage case. It can effectively characterize the combination of changes in mass, damping and stiffness simultaneously.
- The dynamic ISR method applied in a SDOF provides better performance in mass change identification than damping and stiffness detection. The error between the calculated values and actual values of the mass indices are very low.
- Because of the use of the linear squares method, the accuracy of the calculation can be improved by increasing the number of the samples cases and output steps of the data (Table A.1 to Table A.21).
- The accuracy of the results largely depends on the precision of the data. This problem can be easily solved in simulation by increasing the number of significant digits, but in practice, high precision sensors are necessary.

CHAPTER IV

MULTI-DEGREE OF FREEDOM

4.1 Overview of dynamic of ISR Method for MDOF System

4.1.1 Introduction

As presented in Chapter III, dynamic ISR Method is very capable in a SDOF system. The basic theory of dynamic ISR emphasizes the internal stress resultants are not affected by damage at any given section of the structure member. In essence, this theory is not limited to different types of systems. Therefore, the dynamic ISR will be suitable for Multi-degree of freedom (MDOF) systems. Compared with SDOF system, a MDOF system can provide more damage locations, which helps to effectively test whether the proposed method meet the requirements of a Level III method. Additionally, a general approach for MDOF will be presented, which will help to simplify the theory and allow it to be widely used in different cases.

4.1.2 General Approach

For a MDOF system, the model can be taken as a multi-degree of freedom mass-damping-spring system, which is shown in Figure IV.1.

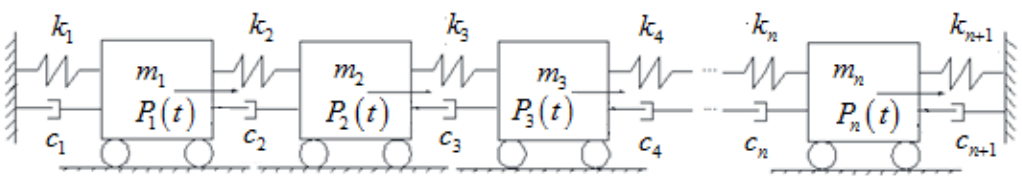

Figure IV.1 Mass-damping-stiffness multi-degree of freedom system model

In order to get a general solution for the MDOF system, the i^{th} member, which is shown in Figure IV.2, is the focus. For the i^{th} member, the mass for initial and final system are m_i and m_i^*. The damping and stiffness, on the left side of the respective mass, for pre-damaged system is c_i, and k_i and for the post-damaged system, is c_i^* and k_i^*. For the right side of the mass, the damping and stiffness for pre-damaged system is c_{i+1} and k_{i+1} and for the post-damaged system, is c_{i+1}^* and k_{i+1}^*. The stress resultants for the pre-damage system and post-damage system both are $p_i(t)$ (Figure IV.3). Based on the assumption of invariant stress resultants, the external dynamic forces for both cases are the same, $P_i(\mathrm{t}) = \hat{P}_i \cos \omega \mathrm{t}$, where $\hat{P}$ is the amplitude of the dynamic force. Those values of the above parameters are unknown.

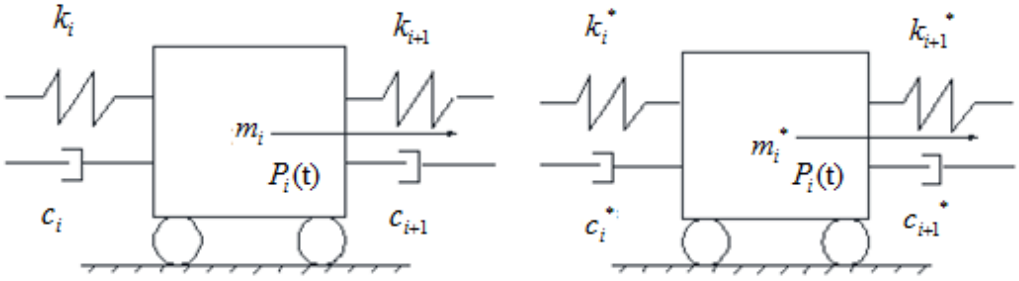

Figure IV.2 The i^{th} member for pre-damage and post-damage cases

The equation of motion for the undamaged system:

$$m_i\ddot{x}_i + c_i\left(\dot{x}_i - \dot{x}_{i-1}\right) + c_{i+1}(\dot{x}_{i+1} - \dot{x}_i) + k_i(x_i - x_{i-1}) + k_{i+1}(x_{i+1} - x_i) = P\left(t\right) \qquad (4.1)$$

Similarly, for the damaged system,

$$m_i^*\ddot{x}_i^* + c_i^*\left(\dot{x}_i^* - \dot{x}_{i-1}^*\right) + c_{i+1}^*(\dot{x}_{i+1}^* - \dot{x}_i^*) + k_i^*(x_i^* - x_{i-1}^*) + k_{i+1}^*(x_{i+1}^* - x_i^*) = P\left(t\right) \quad (4.2)$$

It is assumed that the initial acceleration $\ddot{x}$, velocity $\dot{x}$, displacement x and damaged acceleration $\ddot{x}^*$, velocity $\dot{x}^*$, displacement x^* are known at a specific time. Because $P_i\left(t\right)$ is a function of time, the acceleration, velocity and displacement for both cases are functions of time.

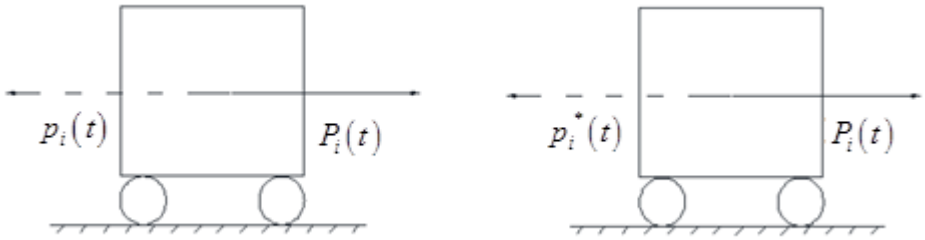

Figure IV.3 Stress resultants and external force in initial and final systems

In the i^{th} member, the potential damage is expressed as a local decrease in mass, damping and stiffness in the structural member. At the cross-section, the consequence of the stress resultants shows as the external force in global coordinates (Figure IV.3). As mentioned in the assumption, the external loading in both pre-damage and post-damage are the same. Based on this relationship, equations in global coordinates can be established to show the results of invariant stress resultants in the local coordinates.

Thus, by equating Eq. (4.1) and Eq. (4.2),

$$\begin{aligned} & m_i\ddot{x}_i + c_i\left(\dot{x}_i - \dot{x}_{i-1}\right) + c_{i+1}(\dot{x}_{i+1} - \dot{x}_i) + k_i(x_i - x_{i-1}) + k_{i+1}(x_{i+1} - x_i) = m_i^*\ddot{x}_i^* \\ & + c_i^*\left(\dot{x}_i^* - \dot{x}_{i-1}^*\right) + c_{i+1}^*(\dot{x}_{i+1}^* - \dot{x}_i^*) + k_i^*(x_i^* - x_{i-1}^*) + k_{i+1}^*(x_{i+1}^* - x_i^*) \end{aligned} \tag{4.3}$$

$$\begin{aligned} & \frac{m_i}{k_{i+1}^*}\ddot{x}_i + \frac{c_i}{k_{i+1}^*}\left(\dot{x}_i - \dot{x}_{i-1}\right) + \frac{c_{i+1}}{k_{i+1}^*}(\dot{x}_{i+1} - \dot{x}_i) + \frac{k_i}{k_{i+1}^*}(x_i - x_{i-1}) + \frac{k_{i+1}}{k_{i+1}^*}(x_{i+1} - x_i) \\ & = \frac{k_i^*}{k_{i+1}^*}\ddot{x}_i^* + \frac{c_i^*}{k_{i+1}^*}\left(\dot{x}_i^* - \dot{x}_{i-1}^*\right) + \frac{c_{i+1}^*}{k_{i+1}^*}(\dot{x}_{i+1}^* - \dot{x}_i^*) + \frac{k_i^*}{k_{i+1}^*}(x_i^* - x_{i-1}^*) + (x_{i+1}^* - x_i^*) \end{aligned} \tag{4.4}$$

Assuming $t = t_1$, Eq. (4.4) can be written as

$$\begin{aligned} & \beta_1\ddot{x}_i(t) - \beta_2\ddot{x}_i^*(t) + \beta_3\left(\dot{x}_i(t) - \dot{x}_{i-1}(t)\right) - \beta_4\left(\dot{x}_i^*(t) - \dot{x}_{i-1}^*(t)\right) \\ & + \beta_5\left(\dot{x}_{i+1}(t) - \dot{x}_i(t)\right) - \beta_6\left(\dot{x}_{i+1}^*(t) - \dot{x}_i^*(t)\right) + \beta_7\left(x_i(t) - x_{i-1}(t)\right) \\ & - \beta_8\left(x_i^*(t) - x_{i-1}^*(t)\right) + \beta_9\left(x_{i+1}(t) - x_i(t)\right) = \left(x_{i+1}^*(t) - x_i^*(t)\right) \end{aligned} \tag{4.5}$$

where,

$$\beta_1 = \frac{m_i}{k_{i+1}^*} \tag{4.6}$$

$$\beta_2 = \frac{m_i^*}{k_{i+1}^*} \tag{4.7}$$

$$\beta_3 = \frac{c_i}{k_{i+1}^*} \tag{4.8}$$

$$\beta_4 = \frac{c_i^*}{k_{i+1}^*} \tag{4.9}$$

$$\beta_5 = \frac{c_{i+1}}{k_{i+1}^*} \tag{4.10}$$

$$\beta_6 = \frac{c_{i+1}^*}{k_{i+1}^*} \tag{4.11}$$

$$\beta_7 = \frac{k_i^*}{k_{i+1}^*} \tag{4.12}$$

$$\beta_8 = \frac{k_i^*}{k_{i+1}^*} \tag{4.13}$$

$$\beta_9 = \frac{k_{i+1}}{k_{i+1}^*} \tag{4.14}$$

Thus the damage indices are,

$$\beta_{m_i} = \frac{m_i}{m_i^*} = \frac{\beta_1}{\beta_2} \tag{4.15}$$

$$\beta_{c_i} = \frac{c_i}{c_i^*} = \frac{\beta_3}{\beta_4} \tag{4.16}$$

$$\beta_{c_{i+1}} = \frac{c_{i+1}}{c_{i+1}^*} = \frac{\beta_5}{\beta_6} \tag{4.17}$$

$$\beta_{k_1} = \frac{k_i}{k_i^*} = \frac{\beta_7}{\beta_8} \tag{4.18}$$

$$\beta_{k_{i+1}} = \frac{k_{i+1}}{k_{i+1}^*} = \beta_9 \tag{4.19}$$

The damage severities are,

$$\alpha_{m_i} = \frac{1}{\beta_{m_i}} - 1 \tag{4.20}$$

$$\alpha_{c_i} = \frac{1}{\beta_{c_i}} - 1 \tag{4.21}$$

$$\alpha_{c_{i+1}} = \frac{1}{\beta_{c_{i+1}}} - 1 \tag{4.22}$$

$$\alpha_k = \frac{1}{\beta_k} - 1 \tag{4.23}$$

$$\alpha_{k_{i+1}} = \frac{1}{\beta_{k_{I+1}}} - 1 \tag{4.24}$$

Using the linear square method to determine the values of the damage indices and severities will increase solution accuracy.

4.2 Simulation procedure for Two degree of freedom System

In order to verify the application of the dynamic ISR method general approach for MDOF, a 2-DOF model has been built in SAP2000 (Figure IV.4 and Figure IV.5).

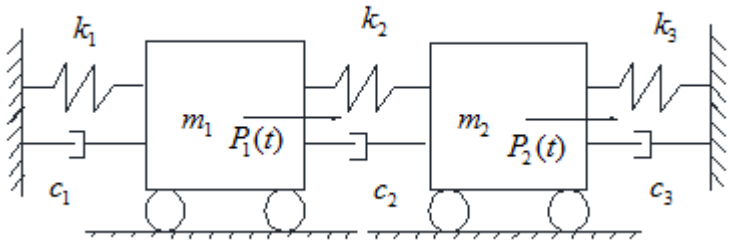

Figure IV.4 Two degree of freedom system model for undamaged case

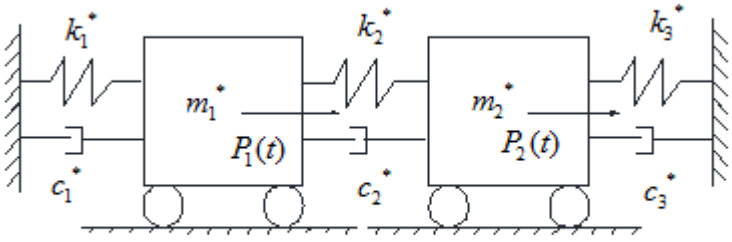

Figure IV.5 Two degree of freedom system model for damaged case

From the Figure IV.4 and Figure IV.5, the pre-damage model contains two particles and three link supports, which can be taken as damping and stiffness. By decreasing the values of the particles mass and the coefficient of the links, post-damage model can be developed. The dynamic load $P_1(t)$ was applied to the first particle and $P_2(t)$ to the second particle for both initial and final systems.

For the 2-DOF system, multiple types of damages and multiple damage locations can be applied. These different damages include reduction of the mass, damping and stiffness. Twelve different combinations have been designed, which can be summarized in Table IV.1.

As mentioned in the general approach of MDOF, the simulation procedure mainly focus on the structural members. Therefore, the results for i^{th} member just provides the changes of the parameters related to itself.

The acceleration, velocity and displacement for initial and final system can be calculated directly by dynamic analysis using SAP2000. Using the data from the finite element program, the damage indices and damage severity can be calculated. The actual values for damage indices and damage severity for each case are listed in the Table IV.2.

Table IV.1 Description of different damage cases

	Mass (kip-s^2)/in		Damping (kip-s/in)			Stiffness (kip/in)			Force Amplitude (kips)	
Number	1	2	1	2	3	1	2	3	1	2
Initial	3.00	2.00	1.50	1.40	1.30	1.00	1.10	1.20	10.00	8.00
Case 1	2.70	2.00	1.50	1.40	1.30	1.00	1.10	1.20	10.00	8.00
Case 2	3.00	1.78	1.50	1.40	1.30	1.00	1.10	1.20	10.00	8.00
Case 3	3.00	2.00	1.43	1.40	1.30	1.00	1.10	1.20	10.00	8.00
Case 4	3.00	2.00	1.50	1.32	1.30	1.00	1.10	1.20	10.00	8.00
Case 5	3.00	2.00	1.50	1.40	1.21	1.00	1.10	1.20	10.00	8.00
Case 6	3.00	2.00	1.50	1.40	1.30	0.88	1.10	1.20	10.00	8.00
Case 7	3.00	2.00	1.50	1.40	1.30	1.00	0.96	1.20	10.00	8.00
Case 8	3.00	2.00	1.50	1.40	1.30	1.00	1.10	1.03	10.00	8.00
Case 9	2.70	1.78	1.43	1.32	1.21	1.00	1.10	1.20	10.00	8.00
Case 10	3.00	2.00	1.43	1.32	1.21	0.88	0.96	1.03	10.00	8.00
Case 11	2.70	1.78	1.50	1.40	1.30	0.88	0.96	1.03	10.00	8.00
Case 12	2.70	1.78	1.43	1.32	1.21	0.88	0.96	1.03	10.00	8.00

Table IV.2 The actual values for damage indicators

	m_1		m_2		c_1		c_2		c_3		k_1		k_2		k_3	
No.	β_{m_1}	α_{m_1}	β_{m_2}	α_{m_2}	β_{c_1}	α_{c_1}	β_{c_2}	α_{k_1}	β_{c_3}	α_{k_3}	β_{k_1}	α_{k_1}	β_{k_2}	α_{k_2}	β_{k_3}	α_{k_3}
1	1.11	-0.10	1.00	0.00	1.00	0.00	1.00	0.00	1.00	0.00	1.00	0.00	1.00	0.00	1.00	0.00
2	1.00	0.00	1.12	-0.11	1.00	0.00	1.00	0.00	1.00	0.00	1.00	0.00	1.00	0.00	1.00	0.00
3	1.00	0.00	1.00	0.00	1.05	-0.05	1.00	0.00	1.00	0.00	1.00	0.00	1.00	0.00	1.00	0.00
4	1.00	0.00	1.00	0.00	1.00	0.00	1.06	-0.06	1.00	0.00	1.00	0.00	1.00	0.00	1.00	0.00
5	1.00	0.00	1.00	0.00	1.00	0.00	1.00	0.00	1.08	-0.07	1.00	0.00	1.00	0.00	1.00	0.00
6	1.00	0.00	1.00	0.00	1.00	0.00	1.00	0.00	1.00	0.00	1.14	-0.12	1.00	0.00	1.00	0.00
7	1.00	0.00	1.00	0.00	1.00	0.00	1.00	0.00	1.00	0.00	1.00	0.00	1.15	-0.13	1.00	0.00
8	1.00	0.00	1.00	0.00	1.00	0.00	1.00	0.00	1.00	0.00	1.00	0.00	1.00	0.00	1.16	-0.14
9	1.11	-0.10	1.12	-0.11	1.05	-0.05	1.06	-0.06	1.08	-0.07	1.00	0.00	1.00	0.00	1.00	0.00
10	1.11	-0.10	1.12	-0.11	1.00	0.00	1.00	0.00	1.00	0.00	1.14	-0.12	1.15	-0.13	1.16	-0.14
11	1.00	0.00	1.00	0.00	1.05	-0.05	1.06	-0.06	1.08	-0.07	1.14	-0.12	1.15	-0.13	1.16	-0.14
12	1.11	-0.10	1.12	-0.11	1.05	-0.05	1.06	-0.06	1.08	-0.07	1.14	-0.12	1.15	-0.13	1.16	-0.14

4.3 Results for Two Degree of Freedom System

By using the calculated data from finite element program, the damage indices and damage severities can be determined. Table IV.3, Table IV.4 and Table IV.5 provide the calculated damage indices for mass, damping and stiffness. Table IV.6, Table IV.7 and Table IV.8 provide the calculated damage severities for mass, damping and stiffness.

Comparing the results of twelve cases in Table IV.3, Table IV.4 and Table IV.5, the dynamic ISR method can detect the exact value of damage indices in 2-DOF system. Most of the percent errors are less than the standard percent error, 2%. By reading the data of the damage indices, potential damage locations are clearly seen. And by reading the value of damage severity, it is easy to get the value of the reduction of each parameters.

Compared to damage indices, the values of damage severity shows the state of the structure more effectively. Using the data in Table IV.6, Table IV.7 and Table IV.8, it is easy to learn the reduction of the parameters in each case. Most of the values of the calculated absolute error are less than 0.02, which shows the effectiveness of the proposed method. By comparing the results, multiple damage location cases can be detected.

It should be noted that the results of damage severities between mass, damping and stiffness, the errors for mass detection are smaller. In the general approach, a concerned member contains a particle and two links. And these links are shared with other members. Therefore, the shared links will have two groups of results from the simulation of the related members. Using the average of the two groups of data will

improve the accuracy of the results at the respective link support. Some related tables can be seen in the Appendix B, and the list results for β_{c_2} , α_{c_2} , β_{k_2} , α_{k_2} in Table IV.6 to Table IV.8 are the mean values.

Table IV.3 Results for mass damage indices

Damage Case	$\beta_{m_1} = m_1 / m_1^*$		$\beta_{m_2} = m_2 / m_2^*$	
	Calc. Value	Percent Error	Calc. Value	Percent Error
Case 1	1.11	1.36E-03	1.00	4.49E-03
Case 2	1.00	-2.67E-04	1.12	5.83E-04
Case 3	1.00	-1.9E-03	1.00	1.84E-02
Case 4	1.00	1.99E-01	1.00	7.83E-02
Case 5	1.00	1.54E-02	1.00	3.32E-03
Case 6	1.00	3.13E-03	1.00	5.28E-03
Case 7	1.00	3.89E-02	1.00	2.37E-02
Case 8	1.00	3.44E-03	1.00	4.45E-03
Case 9	1.11	4.24E-04	1.12	6.40E-04
Case 10	1.11	4.24E-04	1.12	9.95E-05
Case 11	1.00	3.25E-03	1.00	4.27E-04
Case 12	1.11	4.24E-04	1.12	1.16E-04

Notes: (1) The output time step number is 100
(2) The size of the time step is 0.05

Table IV.4 Results for damping damage indices

Damage Case	$\beta_{c_1} = c_1 / c_1^*$		$\beta_{c_2} = c_2 / c_2^*$		$\beta_{c_3} = c_3 / c_3^*$	
	Calc. Value	Percent Error	Calc. Value	Percent Error	Calc. Value	Percent Error
Case 1	1.00	5.13E-02	1.00	4.54E-02	1.00	5.13E-02
Case 2	1.00	2.35E-02	1.00	-2.90E-01	1.00	-1.76E-04
Case 3	1.05	-1.51E-01	1.00	-2.84E-02	1.00	-1.95E-01
Case 4	1.00	-1.64E-01	1.07	-2.13E-01	1.00	5.66E-02
Case 5	1.01	9.00E-01	1.04	4.07E-00	1.07	1.14E-01
Case 6	1.00	3.74E-01	0.99	-1.43E00	1.00	1.07E-01
Case 7	1.00	4.59E-01	1.01	1.23E00	1.00	6.52E-02
Case 8	1.00	5.3E-02	1.00	4.54E-02	1.00	4.49E-03
Case 9	1.05	5.20E-03	1.06	-3.03E-01	1.08	7.02E-02
Case 10	1.00	1.43E-02	1.00	-1.35E-01	1.00	5.22E-02
Case 11	1.05	5.58E-04	1.06	-6.13E-01	1.08	1.91E-01
Case 12	1.05	2.97E-02	1.06	-1.27E-01	1.08	2.41E-03

Notes: (1) The output time step number is 100
(2) The size of the time step is 0.05

Table IV.5 Results for stiffness damage indices for twelve cases

Damage Case	$\beta_{k_1} = k_1 / k_1^*$		$\beta_{k_2} = k_2 / k_2^*$		$\beta_{k_3} = k_3 / k_3^*$	
	Calc. Value	Percent Error	Calc. Value	Percent Error	Calc. Value	Percent Error
Case 1	1.00	6.64E-01	1.00	5.93E-06	1.00	5.66E-01
Case 2	1.00	6.26E-04	1.00	-3.16E-01	1.00	-3.23E-02
Case 3	1.05	2.9E-01	1.00	-1.81E-01	1.00	-2.66E-03
Case 4	1.00	5.90E-01	0.94	-5.72E-00	1.00	-7.92E-02
Case 5	0.99	1.00E00	1.07	6.84E00	1.00	3.88E-01
Case 6	1.13	8.41E-01	0.97	-3.23E-01	1.00	1.34E-02
Case 7	0.99	5.89E-01	1.17	2.13E00	1.00	1.77E-01
Case 8	0.99	6.64E-01	1.00	8.29E-01	1.16	-1.21E-03
Case 9	1.00	6.96E-03	1.00	-3.02E-01	1.00	8.75E-02
Case 10	1.14	3.51E-02	1.15	-2.16E-01	1.16	8.54E-02
Case 11	1.14	9.20E-04	1.15	-6.31E-01	1.16	1.52E-01
Case 12	1.14	6.69E-02	1.15	-2.43E-01	1.16	1.72E-03

Notes: (1) The output time step number is 100
(2) The size of the time step is 0.05

Table IV.6 Results of mass damage severity for twelve cases

Damage Case	$\alpha_{m_1} = 1/\beta_{m_1} - 1$		$\alpha_{m_2} = 1/\beta_{m_2} - 1$	
	Calc. Value	Absolute Error	Calc. Value	Absolute Error
Case 1	-0.10	-1.22E-05	0.00	4.49E-05
Case 2	0.00	-3.00E-06	-0.11	-5.14E-06
Case 3	0.00	2.00E-05	0.00	1.84E-04
Case 4	0.00	-1.90E-03	0.00	-7.82E-04
Case 5	0.00	1.53E-04	0.00	3.3E-05
Case 6	0.00	3.10E-05	0.00	5.30E-05
Case 7	0.00	3.89E-04	0.00	2.37E-04
Case 8	-0.00	4.32E-03	0.00	4.5E-05
Case 9	-0.10	4.05E-06	-0.11	5.54E-06
Case 10	-0.10	4.05E-06	-0.11	1.58E-06
Case 11	0.00	3.05E-04	0.00	4.00E-06
Case 12	-0.10	4.05E-06	-0.11	1.58E-06

Notes: (1) The output time step number is 100
(2) The size of the time step is 0.05

Table IV.7 Results of damping damage severity for twelve cases

Damage Case	$\alpha_{c_1} = 1/\beta_{c_1} - 1$		$\alpha_{c_2} = 1/\beta_{c_2} - 1$		$\alpha_{c_3} = 1/\beta_{c_3} - 1$	
	Calc. Value	Absolute Error	Calc. Value	Absolute Error	Calc. Value	Absolute Error
Case 1	0.00	5.3E-04	0.00	-4.53E-04	0.00	-5.10E-04
Case 2	0.00	2.35E-04	0.00	-2.09E-03	1.00	1.76E-04
Case 3	-0.05	-1.43E-03	0.05	-5.00-03	1.05	-1.95E-03
Case 4	0.00	-1.63E-03	-0.06	2.01E-03	0.00	5.66E-04
Case 5	0.00	8.91E-03	-0.04	3.91E-02	-0.07	1.06E-03
Case 6	0.00	3.76E-03	0.01	1.46E-02	0.00	1.08E-03
Case 7	0.00	4.57E-03	0.00	1.23E00	0.00	6.52E-04
Case 8	0.00	5.34E-04	0.00	4.53E-04	0.00	5.13E-04
Case 9	-0.05	4.96E-04	-0.06	2.86E-03	-0.07	6.53E-04
Case 10	0.00	1.43E-03	0.00	1.35E-03	0.00	5.23E-04
Case 11	-0.05	4.51E-06	-0.05	5.76E-03	-0.07	1.77E-03
Case 12	-0.05	2.82E-05	-0.05	1.12E-03	-0.07	2.25E-05

Notes: (1) The output time step number is 100
(2) The size of the time step is 0.05

Table IV.8 Results of stiffness damage severity for twelve cases

Damage Case	$\alpha_{k_1} = 1/\beta_{k_1} - 1$		$\alpha_{k_2} = 1/\beta_{k_2} - 1$		$\alpha_{k_3} = 1/\beta_{k_3} - 1$	
	Calc. Value	Absolute Error	Calc. Value	Absolute Error	Calc. Value	Absolute Error
Case 1	0.00	-6.67E-03	0.00	5.93E-06	0.00	-8.16E-03
Case 2	0.00	6.26E-04	0.00	-0.32E-03	0.00	-3.23E-06
Case 3	0.00	-2.94E-03	0.00	-1.80E-03	0.00	-2.66E-03
Case 4	0.00	5.87E-03	0.06	-1.00E-02	0.00	-7.93 E-04
Case 5	0.01	1.01E-02	-0.06	6.40E-02	0.00	3.87E-03
Case 6	-0.11	7.46E-03	0.03	3.33E-02	0.00	1.34E-04
Case 7	0.00	5.92E-03	-0.15	1.59E-02	0.00	1.77E-03
Case 8	0.00	6.69E-03	0.00	8.16E-03	-0.14	2.33E-03
Case 9	0.00	7.00E-05	0.00	3.04E-03	0.00	8.76E-04
Case 10	-0.12	3.10E-04	-0.13	1.69E-03	-0.14	7.36E-03
Case 11	-0.12	8.51E-06	-0.13	4.80E-03	-0.14	1.32E-03
Case 12	-0.12	6.05E-04	-0.13	1.85E-03	-0.14	1.48E-05

Notes: (1) The output time step number is 100
(2) The size of the time step is 0.05

4.4 Simulation procedure for Five Degree of Freedom System

Although, dynamic ISR method can effectively show the damage existence, locations and severities in 2-DOF, it does not stand for all MDOF. In order to further verify the application of the dynamic ISR method general approach for MDOF system, a 5-DOF model has been built in SAP2000 (Figure IV.6 and Figure IV.7).

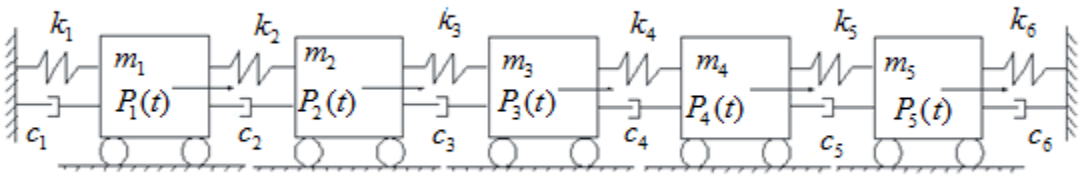

Figure IV.6 Five degree of freedom system model in undamaged case

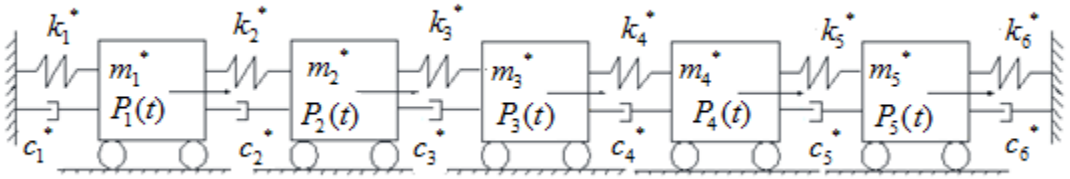

Figure IV.7 Five degree of freedom system model in damaged case

From Figure IV.6 and Figure IV.7, the model contains five particles and six link supports, which can be taken as damping and stiffness. By decreasing the values of the particles mass and coefficient of the links, the post-damage model can be developed. Like the 2-DOF model, multiple types of damages and multiple damage locations can be applied to a 5-DOF model. As mentioned in the general approach of MDOF, the simulation procedure mainly focus on the structural members. Therefore, the results for the i^{th} member just provides the changes of the parameters related to itself

Table IV.9 Description of the damage case for 5-DOF

	undamaged		damaged		Actual Value			
Mass (kip-s^2)/in	m_1	1.00	m_1^*	0.80	β_{m_1}	1.25	α_{m_1}	-0.20
	m_2	2.00	m_2^*	1.62	β_{m_2}	1.23	α_{m_2}	-0.19
	m_3	3.00	m_3^*	2.46	β_{m_3}	1.22	α_{m_3}	-0.18
	m_4	4.00	m_4^*	3.32	β_{m_4}	1.20	α_{m_4}	-0.17
	m_5	5.00	m_5^*	4.20	β_{m_5}	1.19	α_{m_5}	-0.16
Damping (kip-s/in)	c_1	1.10	c_1^*	0.94	β_{c_1}	1.18	α_{c_1}	-0.15
	c_2	1.20	c_2^*	1.03	β_{c_2}	1.16	α_{c_2}	-0.14
	c_3	1.30	c_3^*	1.13	β_{c_3}	1.15	α_{c_3}	-0.13
	c_4	1.40	c_4^*	1.23	β_{c_4}	1.14	α_{c_4}	-0.12
	c_5	1.50	c_5^*	1.34	β_{c_5}	1.12	α_{c_5}	-0.11
	c_6	1.60	c_6^*	1.44	β_{c_6}	1.11	α_{c_6}	-0.10
Stiffness (kip/in)	k_1	2.10	k_1^*	1.91	β_{k_1}	1.10	α_{k_1}	-0.09
	k_2	2.20	k_2^*	2.02	β_{k_2}	1.09	α_{k_2}	-0.08
	k_3	2.30	k_3^*	2.14	β_{k_3}	1.09	α_{k_3}	-0.07
	k_4	2.40	k_4^*	2.26	β_{k_4}	1.06	α_{k_4}	-0.06
	k_5	2.50	k_5^*	2.38	β_{k_5}	1.05	α_{k_5}	-0.05
	k_6	2.60	k_6^*	2.50	β_{k_6}	1.04	α_{k_6}	-0.04

Table IV.10 Dynamic loads for pre-damage and post-damage system

	Undamaged		Damaged		ratio
Force (kips)	$P_1(t)$	$10\cos(2\pi\omega t)$	$P_1^*(t)$	$10\cos(2\pi\omega t)$	1
	$P_2(t)$	$9\cos(2\pi\omega t)$	$P_2^*(t)$	$9\cos(2\pi\omega t)$	1
	$P_3(t)$	$8\cos(2\pi\omega t)$	$P_3^*(t)$	$8\cos(2\pi\omega t)$	1
	$P_4(t)$	$7\cos(2\pi\omega t)$	$P_4^*(t)$	$7\cos(2\pi\omega t)$	1
	$P_5(t)$	$6\cos(2\pi\omega t)$	$P_5^*(t)$	$6\cos(2\pi\omega t)$	1

To avoid repetitive simulation, only one damage case is designed, which contains all types of damages in mass, damping and stiffness at multiples damage locations. The description of every parameter and the actual results is listed in Table IV.9. The applied load is listed in Table IV.10.

4.5 Results for 5-DOF System

Different from the example in the 2-DOF, the simulation for 5-DOF mainly focuses on one damage case, which considers all types of damage at every potential damage location. Table IV.11 provides the calculated values of damage indices, which is the ratio of the parameter before and after damage. Table IV.12 presents the data of calculated damage severity, which indicates the reduction in every parameter. From the two tables, the results show good agreement. The error between the calculated values and the actual values are small.

Table IV.11 Results for damage indices for 5-DOF

Parameter number	$\beta_m = m / m^*$		$\beta_c = c / c^*$		$\beta_k = k / k^*$	
	Calc. Value	Percent Error	Calc. Value	Percent Error	Calc. Value	Percent Error
1	1.25	3.87E-08	1.18	2.02E-05	1.10	1.87E-05
2	1.23	1.89E-07	1.16	-2.61E-06	1.09	-3.62E-06
3	1.22	1.14E-08	1.15	1.15E-05	1.08	7.72E-06
4	1.20	-2.10E-07	1.14	1.97E-05	1.06	1.79E-09
5	1.19	-1.06E-07	1.12	7.71E-04	1.05	2.24E-05
6	-	-	1.11	-1.43E-04	1.04	4.22E-05

Notes: (1) The output time step number is 100
(2) The size of the time step is 0.05

Table IV.12 Results for damage severity for 5-DOF

Parameter number	$\alpha_m = 1/\beta_m - 1$		$\alpha_c = 1/\beta_c - 1$		$\alpha_k = 1/\beta_k - 1$	
	Calc. Value	Absolute Error	Calc. Value	Absolute Error	Calc. Value	Absolute Error
1	-0.20	3.10E-07	-0.15	7.23E-07	-0.09	1.39E-06
2	-0.19	1.53E-07	-0.14	8.90E-05	-0.08	1.94E-06
3	-0.18	9.35E-09	-0.13	1.23E-07	-0.07	7.18E-08
4	-0.17	1.67E-07	-0.12	1.44E-06	-0.06	9.49E-08
5	-0.16	8.90E-08	-0.11	6.34E-06	-0.05	1.02E-06
6	-	-	-0.10	1.29E-06	-0.04	1.55E-06

Notes: (1) The output time step number is 100
(2) The size of the time step is 0.05

The simulation of 5-DOF is based on the results of 2-DOF and proves the correctness of the general approach in the MDOF problems. The dynamic ISR method can not only detect damage but also locate and characterize damages in different locations. It shows the superiority of a Level III non-destructive evaluation methodology in the application of MDOF.

4.6 Conclusion for MDOF System

From the results above, the dynamic ISR method can be applied to a MDOF system for damage detection. The most direct and obvious conclusion of the application in MDOF is that dynamic ISR method can detect different damage locations and be extremely accurate with damage severity. As with the SDOF system, the procedure of the method is straight-forward. Without knowing any parameters or applied loads, the experimental data can solve the problem.

Moreover, one of the improvements in the application is that a general approach has been presented. According to the definition of the ISR, to effectively solve the problem, the whole structural system can be divided into several members. By performing dynamic simulations for the structure member, the experimental data can be calculated automatically from finite element programs. It is not limited to a special model, but can be applied to various structure systems.

However, for the general approach, there are some limitations. Compared the results of the mass, damping and stiffness, it is clear that the detection error in mass is smaller than in damping and stiffness. For mass, the quantity for each member is relatively independent. As for the shared links, these errors come from the discrete

dynamic analysis. But this kind of error can be slightly reduced by overlaping the results from the related members.

Finally, compared to the results of SDOF, the precision of the MDOF results are decreasing, which means high precision data and sensors are still needed for MDOF systems.

CHAPTER V

ROD SYSTEM

5.1 Overview of dynamic ISR Method for Rod System

In Chapter IV, the application for dynamic ISR method was made in discrete-parameter model of structures. However, in reality, all structures are actually three-dimensional solid bodies, and every point in such a body, unless restrained, can displace and rotate along three mutually perpendicular directions x, y, z. In this chapter, continuous models are considered. A finite element based rod structural member model will be picked up to provide "exact" solutions for simple structures. The equation of motion of "one-dimensional" rod system is derived by Newton's Laws.

What follows is an overview of a rod theory. The assumption for the partial-differential-equation model is a long stick, a portion of which is shown in Figure V.1. To derive the equation of motion for axial vibration, a free-body diagram of unit length member is isolated, which is resultant lying along the central axis. A is the cross-section area and ρ is the mass density (i.e., the mass per unit volume). It is assumed that either the member is prismatic (i.e., it has constant cross section) or that its cross section varies only with x, as indicated in Figure V.2.

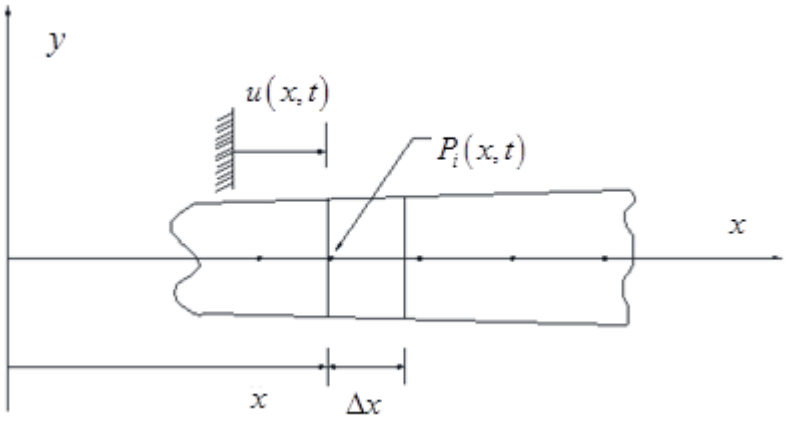

Figure V.1 Portion of a member undergoing axial deformation

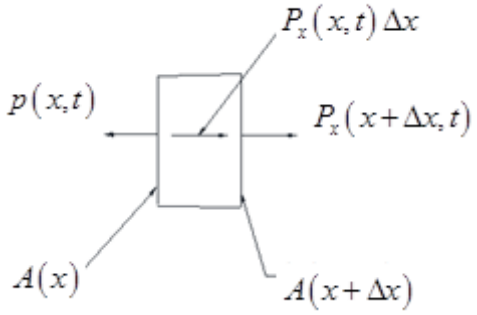

Figure V.2 Free-body diagram of a length-element member

The assumptions for the rod system are the axis of the member remains straight, the material of the system is linearly elastic. The cross sections of the rod remain plane and remain perpendicular to the axis of the member.

Based on these assumptions, the differential equation of motion for axial vibration of a linearly elastic rod is given as:

$$\frac{\partial}{\partial x}\left(AE\frac{\partial u}{\partial x}\right)+p_x(x,t)=\rho A\frac{\partial^2 u}{\partial t^2} \tag{5.1}$$

5.2 Application to Rod System

Based on the theory of the rod system, a free-body diagram of an element length rod member is shown in Figure V.3. It is assumed that either the member is prismatic (i.e., it has constant cross section)

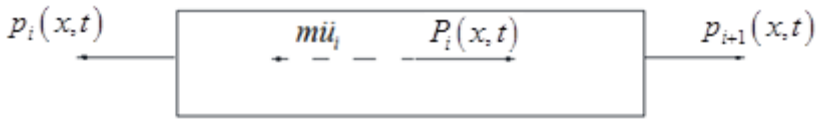

Figure V.3 Free-body diagram for the element length member

In the i^{th} member of the rod, say the acceleration of the unit length member equals to the one at the middle point, which is $\ddot{u}_i$. Here, $\ddot{u}_i$ is used instead of $\ddot{x}_i$ to distinguish the partial differential denominator ∂x. The external force in this member at the center cross section is $P_i(t)$. Based on the free-body diagram, equation of motion of the rod member has been established.

$$P_i(t) + p_{i+1} - p_i = m\ddot{u}_i \tag{5.2}$$

Based on Hooke's law and presented assumptions, the axial force at the i^{th} and $(i+1)^{th}$ cross section the axial force can be defined as p_i and p_{i+1} (Eq. (5.3) and Eq. (5.4)), where the modulus of elasticity for the i^{th} member is E .

$$p_i = EA\left(\frac{\partial u}{\partial x}\right)_i \tag{5.3}$$

$$p_{i+1} = EA\left(\frac{\partial u}{\partial x}\right)_{i+1} \tag{5.4}$$

In terms of the external load

$$m_i\ddot{u}_i + EA\left(\frac{\partial u}{\partial x}\right)_i - EA\left(\frac{\partial u}{\partial x}\right)_{i+1} = P_i(t) \tag{5.5}$$

Similarly, for the damaged system, the equation of motion is,

$$m_i^*\ddot{u}_i^* + (EA)^*\left(\frac{\partial u^*}{\partial x}\right)_i - (EA)^*\left(\frac{\partial u^*}{\partial x}\right)_{i+1} = P_i(t) \tag{5.6}$$

Invoking the stated criterion,

$$m_i\ddot{u}_i + EA\left(\frac{\partial u}{\partial x}\right)_i - EA\left(\frac{\partial u}{\partial x}\right)_{i+1} = m_i^*\ddot{u}_i^* + (EA)^*\left(\frac{\partial u^*}{\partial x}\right)_i - (EA)^*\left(\frac{\partial u^*}{\partial x}\right)_{i+1} \tag{5.7}$$

The later equation reduces to,

$$\frac{m_i\ddot{u}_i}{(EA)^*} - \frac{m_i^*\ddot{u}_i^*}{(EA)^*} + \frac{EA}{(EA)^*}\left(\frac{\partial u}{\partial x}\right)_i - \frac{EA}{(EA)^*}\left(\frac{\partial u}{\partial x}\right)_{i+1} = \left(\frac{\partial u^*}{\partial x}\right)_i - \left(\frac{\partial u^*}{\partial x}\right)_{i+1} \tag{5.8}$$

$$\beta_1\ddot{u}_i - \beta_2\ddot{u}_i^* + \beta_3\left[\left(\frac{\partial u}{\partial x}\right)_i - \left(\frac{\partial u}{\partial x}\right)_{i+1}\right] = \left(\frac{\partial u^*}{\partial x}\right)_i - \left(\frac{\partial u^*}{\partial x}\right)_{i+1} \tag{5.9}$$

For a concerned rod member, the partial differential displacement can be solved by getting the changes of the displacement between the center and double sides of the chosen rod member (Figure V.4).

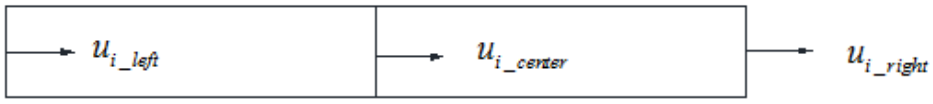

Figure V.4 Axial displacement for the i^{th} member

$$\left(\frac{\partial u}{\partial x}\right)_i - \left(\frac{\partial u}{\partial x}\right)_{i+1} = -u_{i\_left} + 2u_{i\_center} - u_{i\_right} \tag{5.10}$$

$$\left(\frac{\partial u^*}{\partial x}\right)_i - \left(\frac{\partial u^*}{\partial x}\right)_{i+1} = -u_{i\_left}{}^* + 2u_{i\_center}{}^* - u_{i\_right}{}^* \tag{5.11}$$

In which, β_m, β_k are mass damage and stiffness damage indices for the rod member, α_m, α_k are mass damaged and stiffness damage severity for the unit model.

$$\beta_1 = \frac{m_i}{(EA)^*} \tag{5.12}$$

$$\beta_2 = \frac{m_i^*}{(EA)^*} \tag{5.13}$$

$$\beta_3 = \frac{(EA)}{(EA)^*} \tag{5.14}$$

$$\beta_m = \frac{m_i}{m_i^*} = \frac{\beta_1}{\beta_2} \tag{5.15}$$

$$\beta_K = \frac{k_i}{k_i^*} = \beta_3 \tag{5.16}$$

$$\alpha_m = 1/\beta_m - 1 \tag{5.17}$$

$$\alpha_k = 1/\beta_k - 1 \tag{5.18}$$

Using the linear square method to solve for damage indicators and damage severities will decrease the errors.

5.3 Simulation Procedure for Rod System

In order to validate the presented theory for a rod system, a 120ft rod model has been built in SAP2000, which can be designed into pre-damaged case and post-damaged case. The section of the pre-damaged rod is provided in Figure V.5.

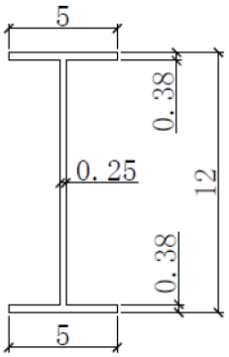

Figure V.5 Section of the rod model

The mass damage severity is defined as the reduction of the value of unit mass. The stiffness damage severity is determined as the changes in Young's modulus. In a certain member, if the damage severity is less than zero, it indicates location of the damage and the value of the damage severity. The rod model is divided into 30 elements, which is shown in Figure V.6. Four different damage cases have been designed based on the changes of the parameters and damage locations (Table V.1).

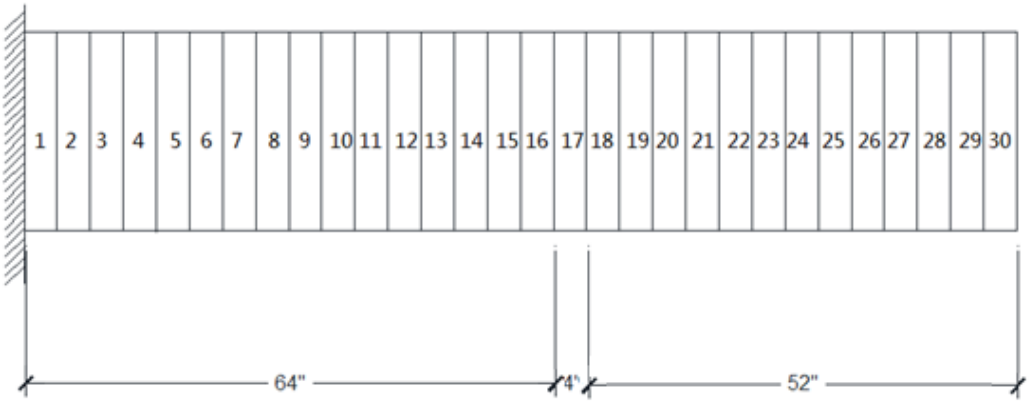

Figure V.6 Finite element mesh of rod system

Table V.1 Damage cases for rod system

	Case	Location	β_m	α_m	β_k	α_k
Single location	1	17^{th}	1.11	-0.10	1.00	0.00
	2	17^{th}	1.00	0.00	1.18	-0.15
	3	17^{th}	1.11	-0.10	1.18	-0.15
Multiple locations	4	17^{th}	1.11	-0.10	1.18	-0.15
		27^{th}	1.25	-0.20	1.22	-0.18

Table V.1 depicts the damage prediction results for four different cases. Case 1 and Case 2 are focusing on the changes of single parameter simulation. Case 3 and Case 4 concern on variable of multi-damage parameters at single locations, include the reduction of the mass and stiffness. Case 4 also involves in multiple damage locations, which is more typical.

5.4 Results for Rod System

Obviously, based on the definition of the dynamic ISR method, this theory can be applied to various types of dynamic loads, such as earthquake and wind. In the simulation process, in order to verify the internal force and external force are always equal. The amplitude of the applied dynamic load $P(t)$ is 10 kips/node and the concerned node is taken as the center of each unit element rod member. The results for four different damage cases will be explained as follows.

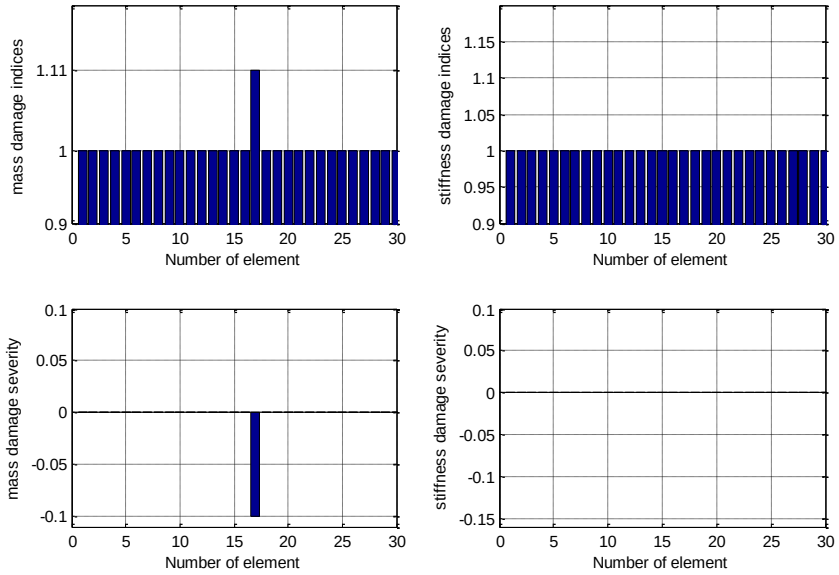

Figure V.7 Calculated damage indicators for Case 1 for rod system

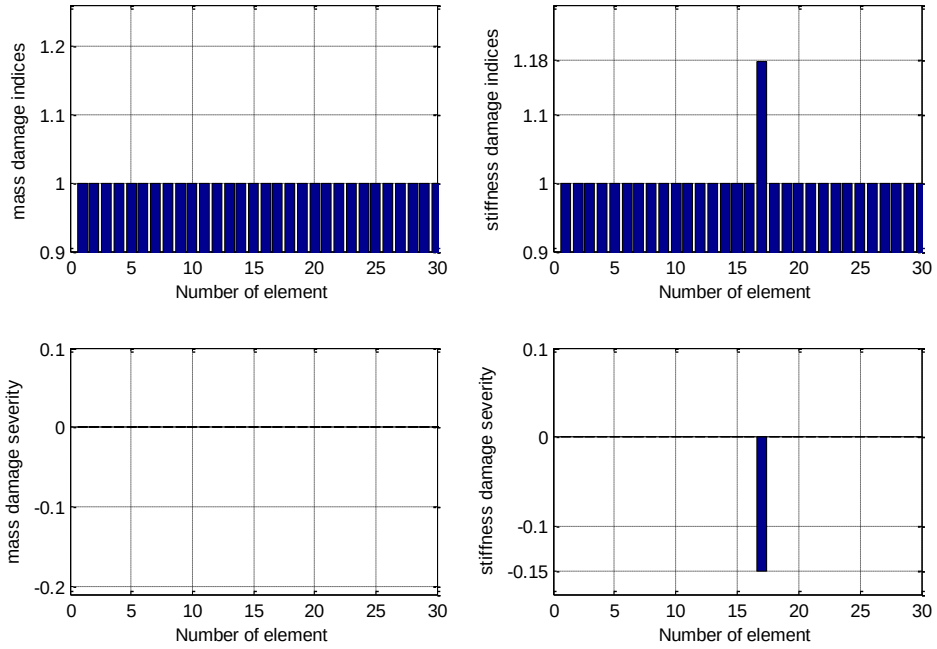

Figure V.8 Calculated damage indicators for Case 2 for rod system

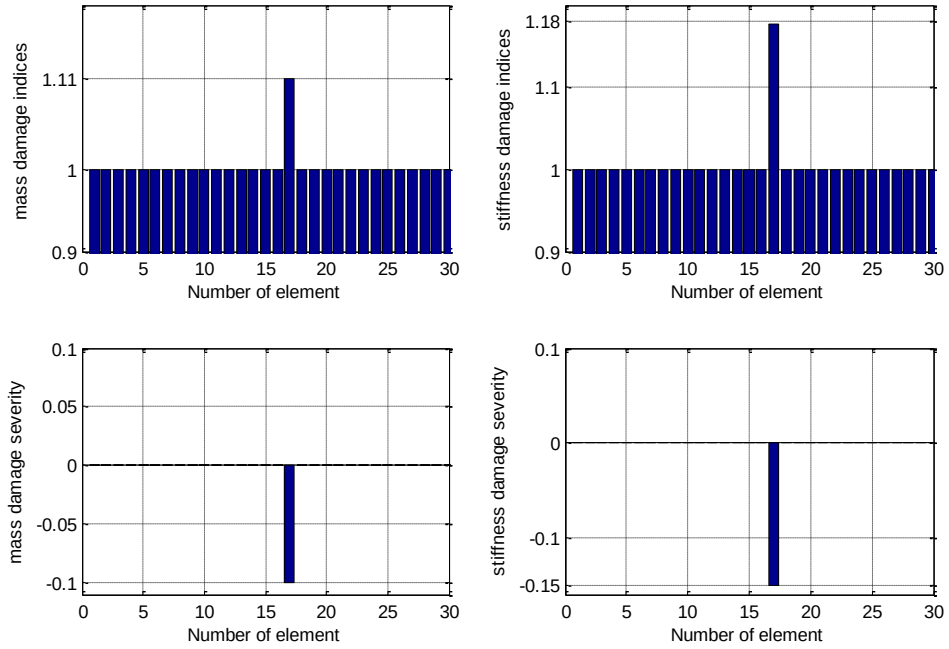

Figure V.9 Calculated damage indicators for Case 3 for rod system

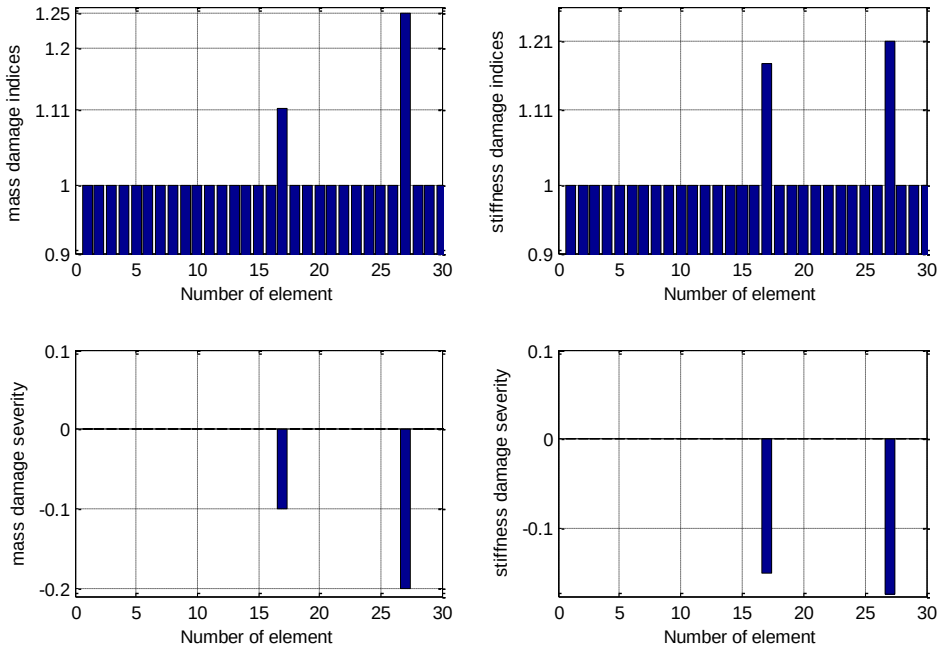

Figure V.10 Calculated damage indicators for Case 4 for rod system

In Figure V.7, it is clear that damage only comes from mass. And the potential damaged area near the 17^{th} member. The mass damage indices and severity can be read directly from Figure V.7, which indicates the reduction of the mass is 10%. The error between calculated damage indicators and the default value is very small. Similarly, for Case 2, Case 3 and Case 4, the existence, the location and the severity of the damage can be clearly shown in the Figure V.8, Figure V.9 and Figure V.10.

5.5 Conclusion for Rod System

For rod system model, it is more typical than the discrete-parameter model, which has been explained in the previous chapters. According to the principle of

dynamic ISR method, the application to the rod model is also based on the finite element method. By doing dynamic analysis for a unit rod member, related the pre-damage and post-damage situation by invariant internal stress. Using the calculated data from finite element program, the ratio of the parameters for each member will be calculated to indicate the state of the structures.

From the simulation results, it is clear that the performance of the damage prediction by dynamic ISR method is very applicable. The advantages in rod simulation are forward the ones in discrete parameter system. From the results of the four different damaged cases, it is an explicit Level III damage detection method which can simultaneously identify the existence, locations and the severities of the damage.

One of the assumption for rod system is that the system is linearly elastic and the cross section is prismatic or varies by x. When applied this method into real situation, the change of the cross section will also impact the results for damage indicators.

Compared to mass-damping-spring system, the rod system is more complicated. The requirement of the data has been improved. In the procedure of the simulation, the number of the output has been increased to 500. Additionally, in order to solve partial differential parameters, it assumes that the unit member have the same damage state. However, in reality, the damage always occurs in a very small area and the severity of the damages can be nonlinearly. On the one hand, if the length of the concerned element member is too large, the correct prediction of damage will not be obtained. On the other hand, if the length of the unit member is very small, in other words, the measuring position is really near, which means the sensor should be placed very closely.

CHAPTER VI

BEAM SYSTEM

6.1 Overview of dynamic ISR Method for Beam System

In the Chapter V, rod model has been set up to prove the accuracy of the dynamic ISR method. However, rod system just stands for models undergo axial deformation. In reality, all structures are actually three-dimensional solid bodies, and every point in such a body, unless restrained, can displace and rotate along three mutually perpendicular directions, x, y, and z. In this chapter, structures models which represent the transverse vibration of beam will be provided. The general example models in this research are taken as Euler-Bernoulli beam. Euler- Bernoulli beam theory covers the case for small deflections of a beam that is subjected to lateral loads only. In the beam model, a finite element based beam structural member will be picked up to provide "exact" solutions for simple structures. The equation of motion of "one-dimensional" Euler-Bernoulli beam system will be derived by Newton's Laws.

6.2 Overview for Euler-Bernoulli Beam System

Euler-Bernoulli beam theory, which is also known as classical beam theory, is a simplified linear theory of elasticity. This theory presents a methodology to calculate the load-carrying and deflection characteristics of beams. Based on the definition mentioned above, the general model for an Euler Bernoulli beam is a long, thin system undergoing transverse vibration.

The equation of motion of Euler-Bernoulli beam system is derived using Newton's Second Law. Figure VI.1 shows a portion of a member undergoing transverse motion (i.e., motion in the y direction), and Figure VI.2 shows an appropriate free-body diagram. The transverse displacement of the point $(x,0)$ on the neutral axis of the beam is labeled as $v(x,t)$, with positive v in the $+y$ direction. The bending moment at section x is $M(x,t)$, the transverse shear force is $S(x,t)$, and the external transverse force per unit length is $P_y(x,t)$, with the sign convention for these specific in Figure VI.2.

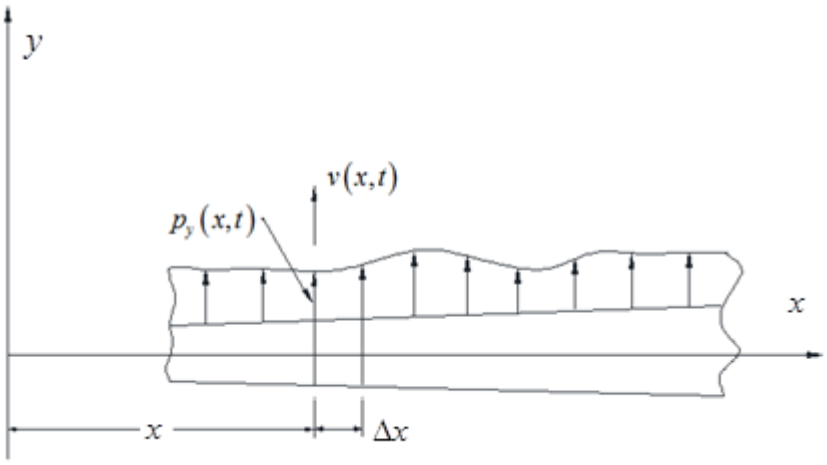

Figure VI.1 Euler-Bernoulli beam model

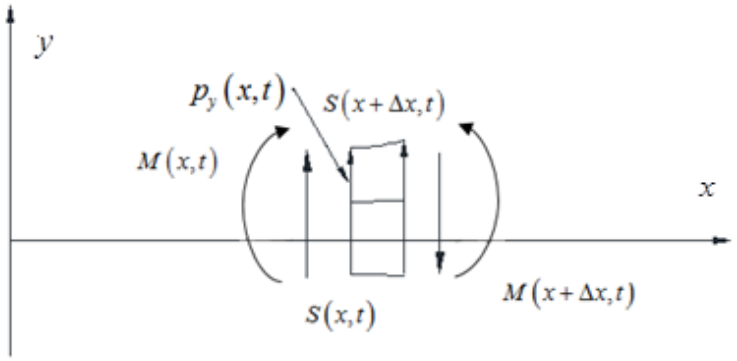

Figure VI.2 Internal force of Euler Bernoulli beam system

The assumptions of Euler- Bernoulli elementary beam theory are:

- The principle plane of the beam is $x-y$ plane, which also remains plane as beam deforms in y-direction.
- The neutral surface for the Euler-Bernoulli beam is the original $x-z$ plan. The neutral axis of the beam, which undergoes on extension or compression, is labeled the x axis.
- Cross section, which are perpendicular to the neutral axis in the undeformed beam, remains plane and remains perpendicular to the deformed neutral axis, that is, transverse shear deformation is neglected.
- The material is linearly elastic and the beam is homogenous at any cross section. (Generally, $E=$ constant throughout the beam.)
- Stresses σ_y and σ_z are negligible compared to σ_x.
- The rotation inertia of the beam may be neglected in the moment equation.

- The mass density, $\rho(x)$, is constant at each cross section, so that the mass center coincides with the centroid of the cross section (Generally, $\rho =$ constant throughout the beam).

From the kinematics on the assumptions, the bending moment can be related to the curvature by the moment-curvature equation (Eq. 6.1), where I is the area moment of inertia of the cross section.

$$M(x,t) = \frac{EI}{\mu} \tag{6.1}$$

Based on the Newton's Laws (Eq. 6.2 to Eq. 6.3), the equation of motion for the unit member can be solved (Eq. 6.4).

$$\sum F_y = \Delta m a_y \tag{6.2}$$

$$\sum M_G = \Delta I_G \alpha \tag{6.3}$$

$$\frac{\partial^2}{\partial x^2}\left(EI \frac{\partial^2 v}{\partial x^2} \right) + \rho A \frac{\partial^2 v}{\partial t^2} = p_y(x,t) \tag{6.4}$$

6.3 Application to Euler-Bernoulli Beam System

In this section, a free-body diagram of an element length Euler-Bernoulli beam member is shown in Figure VI.3. It is assumed that either the member is prismatic (i.e., it has constant cross section). The actual deformation of the beam member is not shown in the picture.

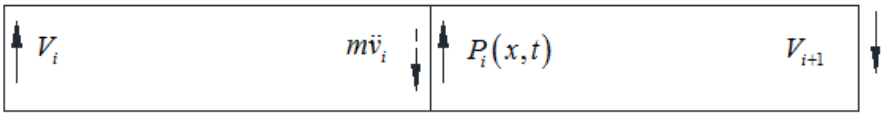

Figure VI.3 Free-body diagram of the Euler-Bernoulli beam member

Based on the description in the above passage and the free-body diagram in Figure VI.3, equation of motion for the member has been set up in Eq. (6.5).

$$P_i(t) - V_{i+1} + V_i = m\ddot{v}_i \tag{6.5}$$

Notes that,

$$V_i(t) = EI\left(\frac{\partial^3 v(x,t)}{\partial x^3}\right)_i \tag{6.6}$$

$$V_{i+1}(t) = EI\left(\frac{\partial^3 v(x,t)}{\partial x^3}\right)_{i+1} \tag{6.7}$$

For the undamaged system, the equation of motion is,

$$m\ddot{v}_i + V_{i+1}(t) - V_i(t) = P(t) \tag{6.8}$$

Similarly, for the damaged system, the equation of motion is,

$$m^*\ddot{v}_i^* + V_{i+1}{}^*(t) - V^*{}_i(t) = P(t) \tag{6.9}$$

Equating Eq. (6.8) and Eq. (6.9),

$$m\ddot{v}_i + V_{i+1}(t) - V_i(t) = m^*\ddot{v}_i^* + V_{i+1}{}^*(t) - V_i^*(t) \tag{6.10}$$

By simplifying Eq. (6.10),

$$
\begin{aligned}
& m_i \frac{\partial^2 v}{\partial t^2} + (EI)_i \left[\frac{\partial^3 v}{\partial x^3}\Big|_{i+1} - \frac{\partial^3 v}{\partial x^3}\Big|_i \right] \\
& -m_i^* \frac{\partial^2 v^*}{\partial t^2} = (EI)_i^* \left[\frac{\partial^3 v^*}{\partial x^3}\Big|_{i+1} - \frac{\partial^3 v^*}{\partial x^3}\Big|_i \right]
\end{aligned} \tag{6.11}
$$

$$
\begin{aligned}
& \beta_4 \frac{\partial^2 v G_i}{\partial t^2} + \beta_5 \left[\frac{\partial^3 v}{\partial x^3}\Big|_{i+1} - \frac{\partial^3 v}{\partial x^3}\Big|_i \right] \\
& -\beta_6 \frac{\partial^2 v^* G_i}{\partial t^2} = \left[\frac{\partial^3 v^*}{\partial x^3}\Big|_{i+1} - \frac{\partial^3 v^*}{\partial x^3}\Big|_i \right]
\end{aligned} \tag{6.12}
$$

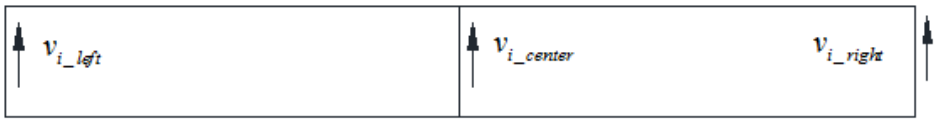

Figure VI.4 Transverse displacement for the i^{th} member

Based on the Figure VI.4, the partial differential equation can be solved as,

$$
\left(\frac{\partial^3 v}{\partial x^3} \right)_{i+1} - \left(\frac{\partial^3 v}{\partial x^3} \right)_i = -\frac{\partial \theta_{i\_left}}{\partial x} + \frac{\left(\frac{\partial v}{\partial x} \right)_{i\_right} - \left(\frac{\partial v}{\partial x} \right)_{i\_left}}{\partial x} - \frac{\partial \theta_{i\_right}}{\partial x} \tag{6.13}
$$

Similarly for undamaged system,

$$
\left(\frac{\partial^3 v^*}{\partial x^3} \right)_{i+1} - \left(\frac{\partial^3 v^*}{\partial x^3} \right)_i = -\frac{\partial \theta_{i\_left}^*}{\partial x} + \frac{\left(\frac{\partial v^*}{\partial x} \right)_{i\_right} - \left(\frac{\partial v^*}{\partial x} \right)_{i\_left}}{\partial x} - \frac{\partial \theta_{i\_right}^*}{\partial x} \tag{6.14}
$$

In which, β_m, β_k are mass damage and stiffness damage indices for the beam member, α_m, α_k are mass damaged and stiffness damage severity for the unit model.

$$\beta_1 = \frac{(EI)_i}{(EI)_i^*} \tag{6.15}$$

$$\beta_2 = \frac{(m)_i}{(EI)_i^*} \tag{6.16}$$

$$\beta_3 = \frac{(m)_i^*}{(EI)_i^*} \tag{6.17}$$

$$\beta_k = \beta_1 \tag{6.18}$$

$$\beta_m = \frac{(m)_i}{(m)_i^*} = \frac{\beta_5}{\beta_6} \tag{6.19}$$

$$\alpha_m = 1/\beta_m - 1 \tag{6.20}$$

$$\alpha_k = 1/\beta_k - 1 \tag{6.21}$$

Using the linear square method to solve for damage indicators and damage severities will decrease the calculated errors.

6.4 Simulation Procedure for Euler-Bernoulli Beam System

In order to verify the presented theory for a beam system, a 60ft simply supported beam model has been built in SAP2000, which can be designed into pre-damaged case and post-damaged case. The cross section of the pre-damaged rod is provided in Figure VI.5.

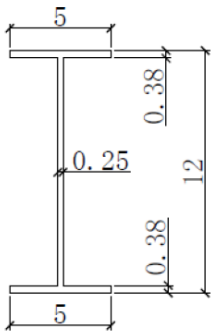

Figure VI.5 Cross-section of the beam model

The mass damage severity is defined as the decreases in volume of the unit mass. The stiffness damage severity is determined as the reduction of Young's modulus. In a certain member, if the damage severity is less than zero, it indicates where the damage exists and the value of the damage severity stands for how much the damage is. The simply supported beam model is divided into 30 elements, which is shown in Figure VI.6. Four different damage cases have been designed based on the changes of the parameters and damage locations (Table V.1).

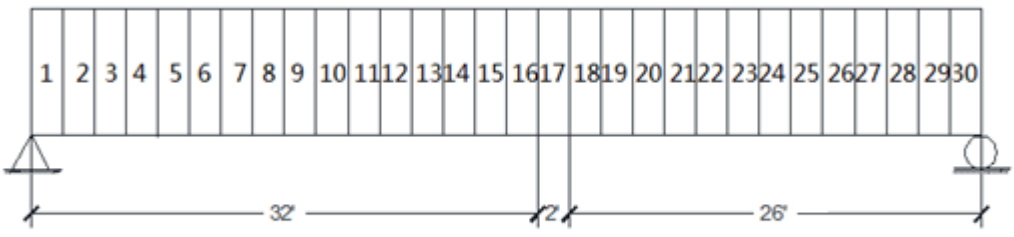

Figure VI.6 Finite element mesh of simply supported beam system

Table VI.1 Damage cases for Euler-Bernoulli beam system

	Case	Location	β_m	α_m	β_k	α_k
Single location	1	17^{th}	1.11	-0.10	1.00	0.00
	2	17^{th}	1.00	0.00	1.18	-0.15
	3	17^{th}	1.11	-0.10	1.18	-0.15
Multiple locations	4	17^{th}	1.11	-0.10	1.18	-0.15
		25^{th}	1.05	-0.05	1.21	-0.18

Table VI.1 Damage cases for Euler-Bernoulli beam system provides the damage prediction results for the designed cases. Case 1 and Case 2 are focusing on the changes of single parameter simulation. Case 3 and Case 4 mainly concern on variable of multi-damage parameters at single locations, including the reduction of the mass and stiffness. Case 4 contains multiple damage locations, which is more typical.

The presented example focuses on simply supported beam. Note that the aspect ratio (depth/length) of the beam is less than $1/10$, which meets with the requirement of the Euler-Bernoulli beam system theory. Additionally, the results of simulation for different boundary condition examples, such as fixed-fixed beam and cantilever beam will be provided in the Appendix.

6.5 Results for Euler-Bernoulli Beam System

Obviously, based on the definition of dynamic ISR method, this theory can be applied to various types of dynamic loads, such as earthquake and wind. In the

simulation process, in order to easily verify the internal force and external force are always equal. The amplitude of the applied dynamic load $P(t)$ is 10 kips/node and the concerned node is taken as the center of each unit element beam member. The direction of the dynamic load is in y direction. And the results for four different damage cases will be explained as follows.

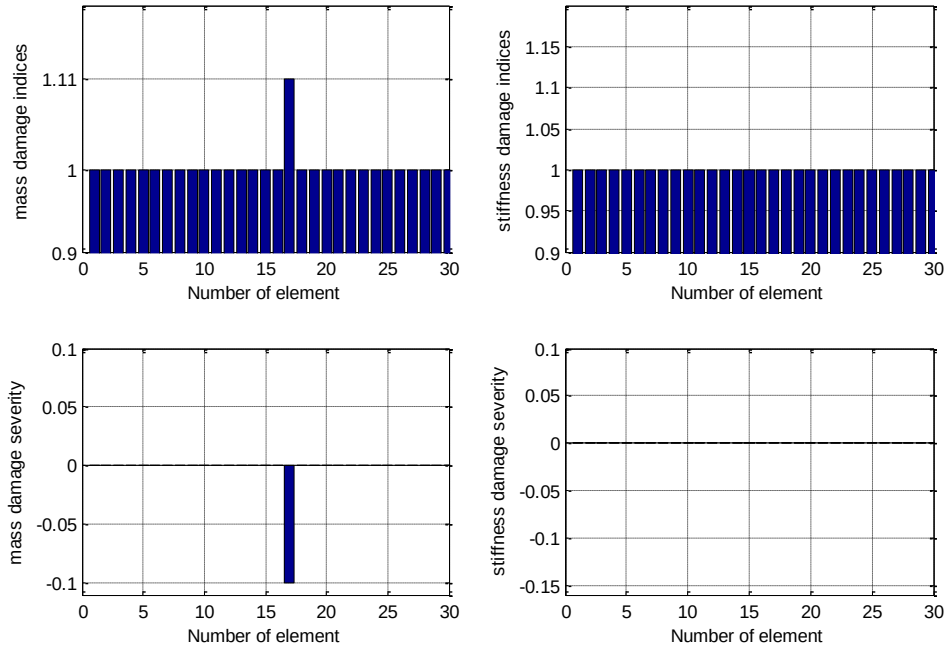

Figure VI.7 Calculated damage indicators for Case 1 for beam system

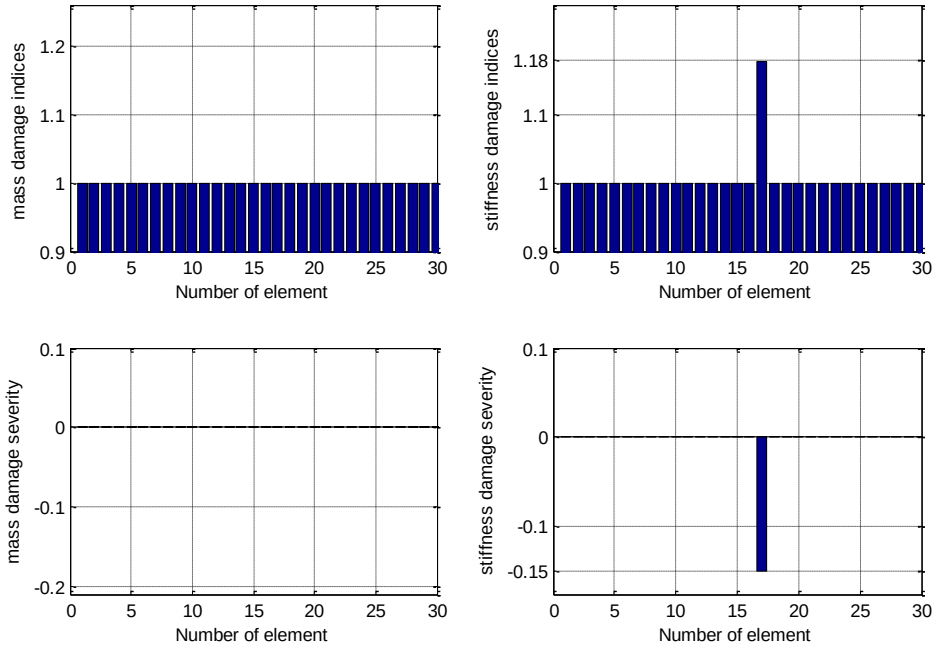

Figure VI.8 Calculated damage indicators for Case 2 for beam system

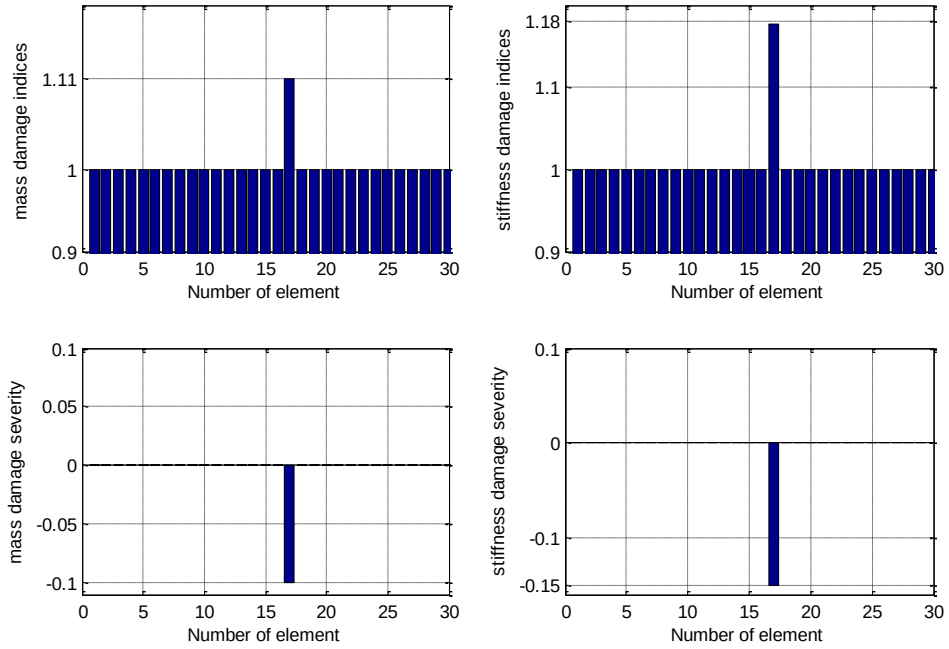

Figure VI.9 Calculated damage indicators for Case 3 for beam system

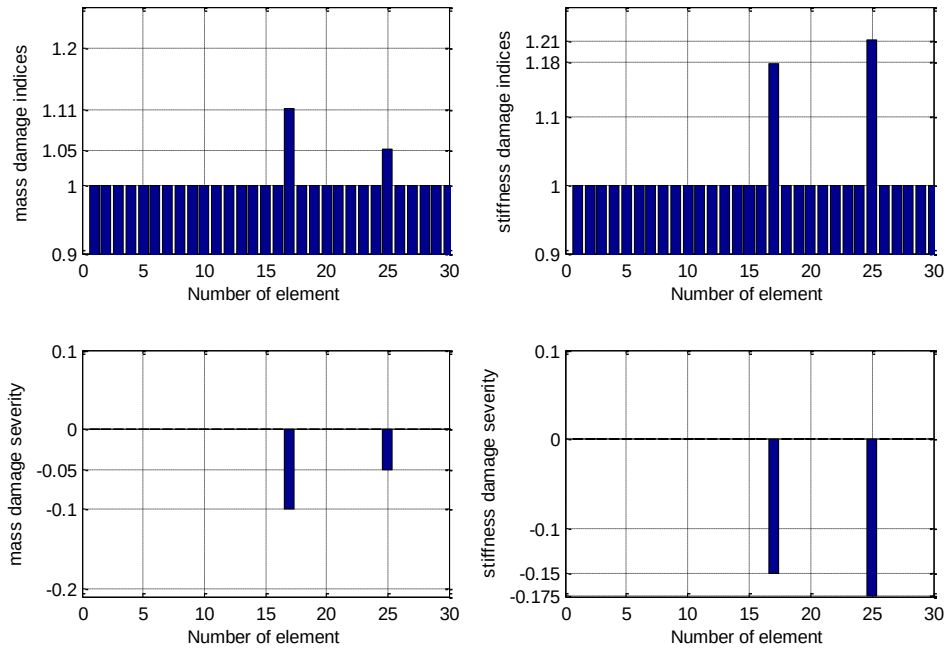

Figure VI.10 Calculated damage indicators for Case 4 for beam system

From the Figure VI.7, Figure VI.8, Figure VI.9 and Figure VI.10, it is clear to see the states of structures. From Case 1 to Case 3, the potential damage location is 17^{th} element. In Case 1, the calculated mass damage severities at 17^{th} unit is -0.10, which indicates the reduction of the mass at near region is 10%. Similarly, the parameter decrease for Case 2 is 15% reduction of stiffness. And Case 3 is the combination case of Case 1 and Case 2. Additionally, for Case 4, the potential damage locations are element 17 and element 25. And the damage severities in Figure VI.10 demonstrates the exact damage states of the structures system. Compared the results read from the above figures and Table VI.1, the predicted states of the structure highly agrees with the designed the ones.

6.6 Conclusions for Beam System

Beam system model undergoes the transverse deformation, which is more typical than rod models. According to the principle of dynamic ISR method, the analysis for the beam model mainly bases on the finite element method. By doing dynamic analysis for a unit beam member, relate the pre-damage and post-damage situation by invariant internal stress. Using the calculated acceleration and displacement from SAP2000, the damage indicators for each unit member will be calculated to predict the state of the structures.

From the simulation results, it is clear that the performance of the damage prediction by dynamic ISR method is very applicable. The advantages in beam simulation are forward the ones in previous chapter. From the results of the four different damaged cases, it is an explicit Level III damage detection method which can simultaneously identify the existence, locations and the severities of the damage. Additionally, the effectiveness of this method is not affected by changing boundary conditions (Table A.31) or combining multiple damage locations.

The assumption for beam system is that the system is linearly elastic and the cross section is prismatic or varies by x . When applied this method in to real situation, the change of the cross section will also impact the results for damage indicators.

The application of the beam system required high precision of the data. In the procedure of the simulation, the number of the output has been increased to 500. Additionally, as mentioned in rod system, in order to solve partial differential parameters, we assume the unit member have the same damage state. However, in

reality, the damage always occurs in a very small area and the severity of the damages can be nonlinearly. The length of the chosen member will apparently impact the results of simulations.

CHAPTER VII

TRUSS SYSTEM

7.1 Overview of dynamic ISR Method for Truss System

Based on the previous work, the dynamic ISR method works well in discrete-parameter models of structures and beam systems. In truss system, the basic idea for dynamic ISR method is also applicable. Thus, it may be able to use the general beam approach to detect damage for every single member. However, a truss system is always composed by several members, it is not smart to identify damage from members to members. Also it is hard to apply dynamic load and get the value of the acceleration and the displacement at the midpoint of the members. Therefore, in this chapter, a direct approach of truss will be used, which is called node method.

The truss has a very restrict definition: It is composed of pin-connected elements which are loaded as only at its joints. (Spillers, 1972) In other words, the resultant member force lies along a straight line between the ends of the member. The member force can be describe as specific single scalar because only forces, no moments acts at the end of the members.

In this chapter, the research only concerned with straight, pin-connected truss system. The truss member are idealized as lines which meet at points which is called joints. The free body diagram of the joint j of a generic truss is depicted as Figure VII.1.

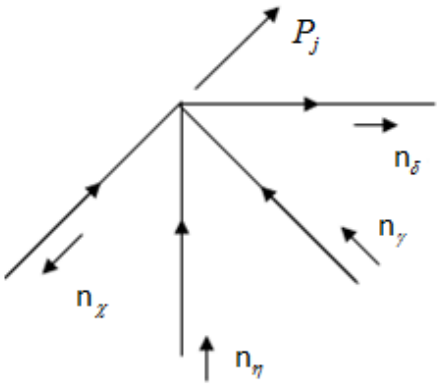

Figure VII.1 j^{th} joint

In a general a joint equilibrium equation must contain a term for each member incident upon the joint –the sign is determined by whether the element is positive or negatively incident. In the Figure VII.1, this precisely form provided by, where i is the number of the truss element and j is the number of joint. χ, η, γ, δ are directions for each element at j^{th} joint.

$$\left(F_\chi n_\chi - F_\eta n_\eta - F_\gamma n_\gamma + F_\delta n_\delta\right)\delta_j + P_j(t) = m_j \alpha_j \tag{7.1}$$

Based on the node method for trusses, the node equilibrium equation become as follows, in which δ is the joints displacement. Δ is the length change of each member. F_i is the member force of the i^{th} element. $P_j(t)$ is the joint force at the j^{th} joint.

$$NF = P \tag{7.2}$$

Using Hooke's Law,

$$F = k\Delta \tag{7.3}$$

The branch-displacement joint-displacement equation,

$$\Delta = N\delta \tag{7.4}$$

For the entire structure k is the primitive stiffness matrix.

$$k = \begin{bmatrix} k_1 & & & & \\ & k_2 & & & \\ & & k_3 & & \\ & & & k_4 & \\ & & & & k_5 \end{bmatrix} \tag{7.5}$$

n_i is the unit vector of the member, N represents the geometrical connectivity of the truss structure.

$$F_\chi \mathsf{n}_\chi - F_\eta \mathsf{n}_\eta - F_\gamma \mathsf{n}_\gamma + F_\delta \mathsf{n}_\delta = p_j = NF \tag{7.7}$$

$$Nk\Delta = p_j \rightarrow NkN\delta = p_j \tag{7.9}$$

Thus Eq. (7.1) can be written as Eq. (7.9).

$$\left(\sum_{i=1}^{n} N_i k_i N_i \right) \delta_j + P_j(t) = m_j \alpha_j \tag{7.10}$$

7.2 Application to Truss System

Assume that two comparable systems exist, pre-damage and post-damage truss system. Both truss systems have the same joint connectivity and are subject to the same external loading at the j^{th} joint. $\ddot{u}_j$, $\ddot{u}_j^*$ are the acceleration at j^{th} joint for initial and final system. u_j, u_j^* are the displacement of the j^{th} joint for pre-damage and post-damage system. However, the masses and stiffness of the elements in the two system are unknown. The equation of motion for the undamaged system is,

$$\left(\sum_{i=1}^{n} N_i k_i N_i\right) u_j + P_j(t) = m_j \ddot{u}_j \tag{7.11}$$

Similarly, for the damaged system, the equation of motion is,

$$\left(\sum_{i=1}^{n} N_i^{*} k_i^{*} N_i^{*}\right) u_j^{*} + P_j(t) = m_j^{*} \ddot{u}_j^{*} \tag{7.12}$$

The fundamental assumption is

$$\left(\sum_{i=1}^{n} N_i^{*} k_i^{*} N_i^{*}\right) u_j^{*} - m_j^{*} \ddot{u}_j^{*} = \left(\sum_{i=1}^{n} N_i k_i N_i\right) u_j - m_j \ddot{u}_j \tag{7.13}$$

$$\left(\sum_{i=1}^{n} N_i^{*} k_i^{*} N_i^{*}\right) u_j^{*} - \left(\sum_{i=1}^{n} N_i k_i N_i\right) u_j + m_j \ddot{u}_j = m_j^{*} \ddot{u}_j^{*} \tag{7.14}$$

For a different truss system the $\sum_{i=1}^{n} N_i k_i N_i$ can be different, the stiffness matrix of the system is decomposed to get the stiffness changes for each related members. For example, for the model of Figure VII.1, Eq. (7.14) becomes,

$$\begin{aligned} &\left(F_\chi \tilde{\mathsf{n}}_\chi - F_\eta \tilde{\mathsf{n}}_\eta - F_\gamma \tilde{\mathsf{n}}_\gamma + F_\delta \tilde{\mathsf{n}}_\delta\right) u_j - \left(F_\chi^{*} \tilde{\mathsf{n}}^{*}_{\chi} - F_\eta^{*} \tilde{\mathsf{n}}^{*}_{\eta} - F_\gamma^{*} \tilde{\mathsf{n}}^{*}_{\gamma}\right) u_j^{*} \\ &- F_\delta^{*} \tilde{\mathsf{n}}^{*}_{\delta} u_j^{*} - m_j \ddot{u}_j = m_j^{*} \ddot{u}_j^{*} \end{aligned} \tag{7.15}$$

$$\begin{aligned} &\left(\beta_1 \mathsf{n}_\chi \tilde{\mathsf{n}}_\chi - \beta_2 \mathsf{n}_\eta \tilde{\mathsf{n}}_\eta - \beta_3 \mathsf{n}_\gamma \tilde{\mathsf{n}}_\gamma + \beta_4 \mathsf{n}_\delta \tilde{\mathsf{n}}_\delta\right) u_j - \left(\beta_5 \mathsf{n}_\chi^{*} \tilde{\mathsf{n}}_\chi^{*} - \beta_6 \mathsf{n}_\eta^{*} \tilde{\mathsf{n}}_\eta^{*}\right) u_j^{*} \\ &- \beta_7 \mathsf{n}_\gamma^{*} \tilde{\mathsf{n}}_\gamma^{*} \delta_j^{*} + \beta_8 \mathsf{n}_\delta^{*} \tilde{\mathsf{n}}_\delta^{*} u_j^{*} - \beta_9 \ddot{u}_j = \ddot{u}_j^{*} \end{aligned} \tag{7.16}$$

in which, $\ddot{u}_j = \begin{pmatrix} (\ddot{u}_j)_x \\ (\ddot{u}_j)_y \end{pmatrix}, \ddot{u}_j^{*} = \begin{pmatrix} (\ddot{u}_j^{*})_x \\ (\ddot{u}_j^{*})_y \end{pmatrix}$, $u_j = \begin{pmatrix} (u_j)_x \\ (u_j)_y \end{pmatrix}$, $u_j^{*} = \begin{pmatrix} (u_j^{*})_x \\ (u_j^{*})_y \end{pmatrix}$

$$\beta_1 = \frac{k_\chi}{m_j^{*}} \tag{7.17}$$

$$\beta_2 = \frac{k_\eta}{m_j^*} \tag{7.18}$$

$$\beta_3 = \frac{k_\gamma}{m_j^*} \tag{7.19}$$

$$\beta_4 = \frac{k_\delta}{m_j^*} \tag{7.20}$$

$$\beta_5 = \frac{k_\chi^*}{m_j^*} \tag{7.21}$$

$$\beta_6 = \frac{k_\eta^*}{m_j^*} \tag{7.22}$$

$$\beta_7 = \frac{k_\gamma^*}{m_j^*} \tag{7.23}$$

$$\beta_8 = \frac{k_\delta^*}{m_j^*} \tag{7.24}$$

$$\beta_9 = \frac{m_j}{m_j^*} \tag{7.25}$$

$$\beta_{m_j} = \beta_9 \tag{7.26}$$

$$\beta_{k_\chi} = \frac{\beta_1}{\beta_5} \tag{7.27}$$

$$\beta_{k_\eta} = \frac{\beta_2}{\beta_6} \tag{7.28}$$

$$\beta_{k_\gamma} = \frac{\beta_3}{\beta_7} \tag{7.29}$$

$$\beta_{k_\delta} = \frac{\beta_4}{\beta_8} \tag{7.30}$$

$$\alpha_{m_j} = \frac{1}{\beta_{m_j}} - 1 \tag{7.31}$$

$$\alpha_{k_\chi} = \frac{1}{\beta_{m_\chi}} - 1 \tag{7.32}$$

$$\alpha_{k_\eta} = \frac{1}{\beta_{k_\eta}} - 1 \tag{7.33}$$

$$\alpha_{k_\gamma} = \frac{1}{\beta_{k_\gamma}} - 1 \tag{7.34}$$

$$\alpha_{k_\delta} = \frac{1}{\beta_{k_\delta}} - 1 \tag{7.35}$$

Eq. (7.13) to Eq. (7.34) present the approach to get the mass indicators at the j^{th} joint , β_{m_j} , α_{m_j} and stiffness indicators for every direction, β_{k_χ} , α_{k_χ} , β_{k_η} , α_{k_η} , β_{k_γ} , α_{k_γ} , β_{k_δ} , α_{k_δ} .

7.3 Simulation Procedure for Truss System

In order to verify the presented theory for a truss system, a model has been built in SAP2000, which can be designed into pre-damaged case and post-damaged case. The geometry information of the truss system is shown in Figure VII.2. The amplitude of the dynamic loads applied at joint 2 is 10kips.

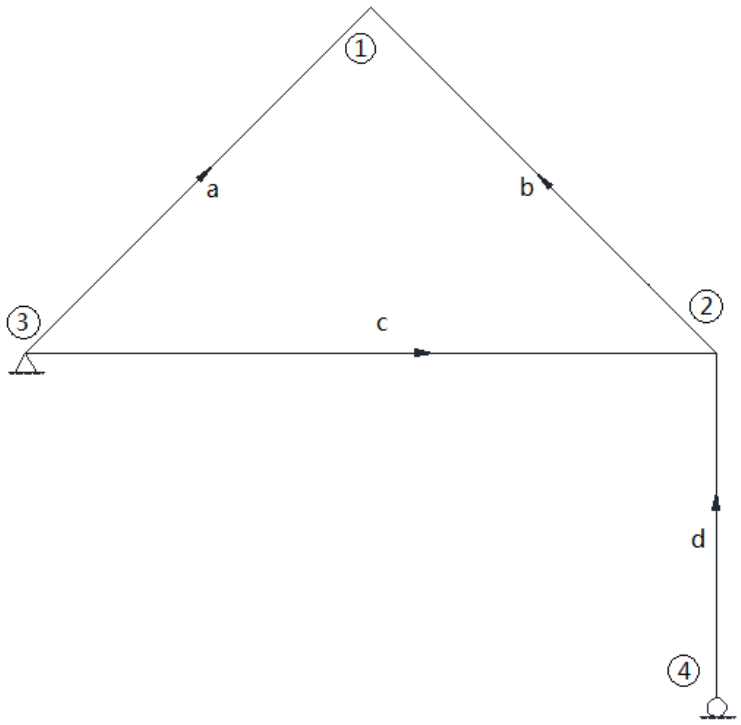

Figure VII.2 Truss Model

The damage cases for truss system will be designed into four different situations. Case 1, Case 2 and Case 3 are mainly focus on single damage location, while Case 4 concerns on multi-damage locations. The designed damaged element is member b for Case 1, 2 and 3. And for Case 4, the damaged locations are member b and member c. Notes that the value of mass at each joint indicates the one at the linked point cross section so that the change of the mass value will indicates the composite results for the related members. The expected damage indices and damage severities results for each cases can be shown in Table VII.4.

Table VII.1 The connectivity information of truss model

Frame text	Joint text (left)	Joint text (right)	Length (in)
a	3	1	108.82
b	2	1	108.82
c	3	2	144.00
d	4	2	72.00

Table VII.2 Damage cases for truss system

Case	β_{m_2}	α_{m_2}	β_{k_b}	α_{k_b}	β_{k_d}	α_{k_d}
1	1.07	-0.06	1.00	0.00	1.00	0.00
2	1.00	0.00	1.11	-0.10	1.00	0.00
3	1.07	-0.06	1.11	-0.10	1.00	0.00
4	1.15	-0.13	1.11	-0.10	1.25	-0.20

7.4 Results for Truss System Simulation

The study for the truss system mainly focus on the 2^{nd} joint of the truss model in Table VII.2. The related detection members are member b, member c and member d. As the designed dynamic load $P_2(t)$ goes horizontally, there is no internal force in member d. Therefore, the changes in stiffness damaged indices and stiffness damage severities will mainly focus on member b and member c.

As mentioned before, the changes of the joint mass indicates the changes to related elements. In other words, the reduction of mass in one element will be expressed as the change versus the composite value for all related elements.

Table VII.3 Results of damage indicators parameter for truss system

Case	$\beta_{m_2} = m_2 / m_2^*$		$\beta_{k_b} = k_b / k_b^*$		$\beta_{k_d} = k_d / k_d^*$	
	Calc. Value	Percent Error	Calc. Value	Percent Error	Calc. Value	Percent Error
1	1.07	-2.24E-07	1.00	-1.87E-06	1.00	4.83E-08
2	1.00	4.12E-07	1.11	-1.84E-07	1.00	-1.80E-07
3	1.07	1.14E-08	1.11	2.51E-07	1.00	-1.87E-07
4	1.15	-2.21E-07	1.11	1.79E-05	1.25	3.28E-08

Table VII.4 Results for damage severities for truss system

Case	$\alpha_{m_2} = 1/\beta_{m_2} - 1$		$\alpha_{k_b} = 1/\beta_{k_b} - 1$		$\alpha_{k_d} = 1/\beta_{k_d} - 1$	
	Calc. Value	Percent Error	Calc. Value	Percent Error	Calc. Value	Percent Error
1	-0.06	-1.75E-09	0.00	-1.90E-08	1.00	4.83E-08
2	0.00	4.00E-09	-0.10	-1.71E-09	1.00	-2.00E-09
3	-0.06	2.26E-05	-0.10	2.34E-09	1.00	-2.00E-09
4	-0.13	6.81E-03	-0.10	1.69E-07	-0.20	7.18E-06

By doing dynamic analysis for joint 2, the time-series based acceleration, displacement can be calculated by SAP2000. Using these data to solve Eq. (7.16), the damage indices and damage severities will be calculated to determine the state of the structures, which can be seen in Table VII.3 and Table VII.4.

In Table VII.3, the damage indices have been calculated for each cases. In Case 1, the reduction of the parameter is the mass at joint 2. In Case 2, the change of the stiffness in element b is 10 %. Case 3 is the combination case of Case 1 and Case 2. As for Case 4, it indicates the potential damage locations are member b and member c. In Table VII.4, it is clearly to see the calculated damage severities in each cases, which can be used to predict the state of the structures. However, the severities of mass for each case can only indicates the changes at the joint cross section. In other words, the results cannot provide the changes of the mass in each member.

7.5 Conclusion for truss system

In this chapter, the application of dynamic ISR in truss system has been introduced. In order to avoid problems by using general approach in beam system, a new direct approach for truss system is provided, which is called node method. (Spillers, 1972) Based on the approach, the truss model has been designed into two cases. One is initial case and the other is final case. By doing dynamic analysis at a certain joint and decomposing of the stiffness matrix, the mass indicators can be calculated at the concerned joints and the damage indicators for each related element.

The results of the simple example for truss system shows great accuracy between the designed and calculated damage indicators. It demonstrates that the dynamic ISR can

be used as a Level III method when applied to the truss system, which can not only provide exact damage locations, but also damage severities.

The advantage for the new approach is that new method can apply dynamic loads at the joints of the truss model. And by using node method it can detect several related elements at the same time. It will definitely save time to find the potential damage regions.

However, one drawback for the node approach is that the change of the mass can be shown as the composite results of every related member. The detailed damage severities for every related element cannot be provided by this method. However, this problem can be solved by comprehensively using the general approach of beam member and node method. In other words, node method can be used to find a potential mass damage joint. Then do a general approach of beam system for each potential elements to get the detailed damage information.

CHAPTER VIII

FRAME SYSTEM

8.1 Overview of Frame System

From Chapter VII, the proposed general approach based on the dynamic ISR method at a certain node has good application for truss system. In order to increase complexity, the plane frame provides a convenient step up from the truss.

The plane frame considered in this chapter is a skeletal structure constructed by assembling plane beams which use rigid connections (Spillers, 1972). The loads are applied at the nodes of the frame system. The frame system model in this chapter does not consider temperature effects, lack of fit. etc. The key difference between plane frames and trusses system is the rigid connection. The boundary condition of the frame system is that both the displacement vector and the rotation are assumed to be zero. The rigid connections allow the adjacent members to restrain the rotations for each other and give rise to moments at the ends of members. At each node of the plane frame model, rotation can be defined as a single scalar, which does not exists in truss systems. It notes that all of the members in the frame is taken as Euler-Bernoulli beam.

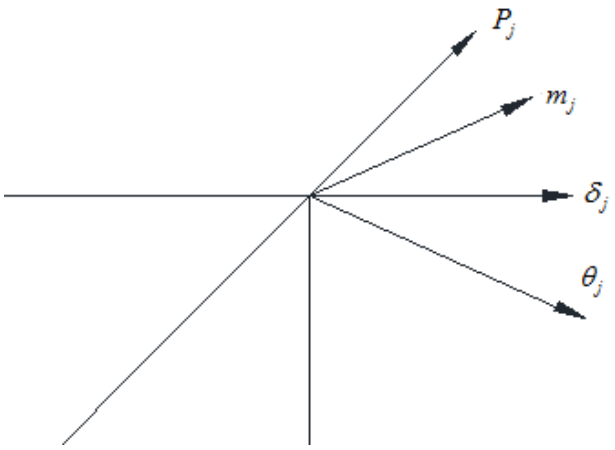

Figure VIII.1 The j^{th} joint of the frame system

Figure VIII.1 depicts a typical frame node associated with the applied dynamic load $P_j(t)$, an applied moment vector m_j, a displacement vector δ_j ., and the rotation vector of the j^{th} node θ_j .

Here, for a plane frame system, displacement vector can be defined as,

$$\delta_j = \begin{bmatrix} (\delta_j)_x \\ (\delta_j)_y \\ \theta_j \end{bmatrix} \tag{8.1}$$

Let f_j^+ and f_j^- represent the end member forces at the positive and negative ends of the j^{th} member.

$$f_i^+ = \tilde{N}_i^+ F_i \text{ and } f_i^- = \tilde{N}_i^- F_i \tag{8.2}$$

$$NF = P_j \tag{8.3}$$

$$F_i = k_i \Delta_i \tag{8.4}$$

Δ_i is the definition of local coordinates. As mentioned in the Chapter VI, it can be taken as Eq. (8.5), where ΔL_i is the length change of the i^{th} member, α_i^+ is the rotation of the positive end and α_i^- is the rotation of the negative end of the i^{th} member.

$$\Delta_i = \begin{bmatrix} \Delta L_i \\ \alpha_i^+ \\ \alpha_i^- \end{bmatrix} = \begin{bmatrix} (\delta_A)_x^{\,i} - (\delta_C)_x^{\,i} \\ \theta_A - \dfrac{1}{L_i}\left[(\delta_A)_y^{\,i} - (\delta_C)_y^{\,i}\right] \\ \theta_C - \dfrac{1}{L_i}\left[(\delta_A)_y^{\,i} - (\delta_C)_y^{\,i}\right] \end{bmatrix} \tag{8.5}$$

For entire structure k is the primitive stiffness matrix.

$$k = \begin{bmatrix} k_1 & & & & & \\ & k_2 & & & & \\ & & k_3 & & & \\ & & & k_4 & & \\ & & & & k_5 & \end{bmatrix} \tag{8.6}$$

N represents the geometrical connectivity of the frame structure.

$$p_j = NF \tag{8.7}$$

$$Nk\Delta = p_j \rightarrow NkN\delta = p_j \tag{8.8}$$

Thus Eq. (8.3) can be written as Eq. (8.9).

$$\left(\sum_{i=1}^{n} N_i k_i N_i\right)\delta_j + P_j(t) = m_j \alpha_j \tag{8.9}$$

8.2 Application to Frame System

Assume that two comparable systems exist, pre-damage and post-damage frame systems. Both systems have the same node connectivity information and are subject to the same external loading at the j^{th} joint. $\ddot{u}_j$, $\ddot{u}_j^*$ are the acceleration at j^{th} joint for initial and final system. u_j, u_j^* are the displacement of the j^{th} joint for pre-damage and post-damage system. However, the values of the mass and stiffness of the elements in two cases are unknown. The equation of motion for undamaged system is,

$$\left(\sum_{i=1}^{n} N_i k_i N_i\right) u_j + P_j(t) = m_j \ddot{u}_j \tag{8.10}$$

Similarly, for damaged system,

$$\left(\sum_{i=1}^{n} N_i^* k_i^* N_i^*\right) u_j^* + P_j(t) = m_j^* \ddot{u}_j^* \tag{8.11}$$

The fundamental assumption is

$$\left(\sum_{i=1}^{n} N_i k_i N_i\right) u_j - m_j \ddot{u}_j = \left(\sum_{i=1}^{n} N_i^* k_i^* N_i^*\right) u_j^* - m_j^* \ddot{u}_j^* \tag{8.12}$$

$$\left(\sum_{i=1}^{n} N_i^* k_i^* N_i^*\right) u_j^* - \left(\sum_{i=1}^{n} N_i k_i N_i\right) u_j - m_j \ddot{u}_j = -m_j^* \ddot{u}_j^* \tag{8.13}$$

in which, $\ddot{u}_j = \begin{pmatrix} (\ddot{u}_j)_x \\ (\ddot{u}_j)_y \\ \ddot{\theta}_j \end{pmatrix}, \ddot{u}_j^* = \begin{pmatrix} (\ddot{u}_j^*)_x \\ (\ddot{u}_j^*)_y \\ \theta_j^* \end{pmatrix}$, $u_j = \begin{pmatrix} (u_j)_x \\ (u_j)_y \\ \theta_j \end{pmatrix}$, $u_j^* = \begin{pmatrix} (u_j^*)_x \\ (u_j^*)_y \\ \theta_j^* \end{pmatrix}$

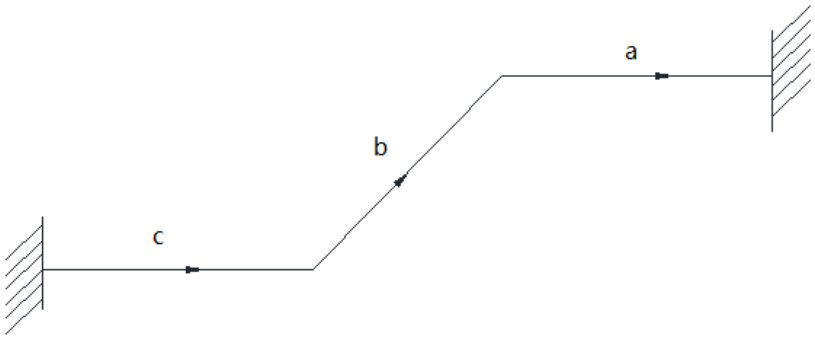

Figure VIII.2 Simple frame system

For different frame systems the matrix of $\sum_{i=1}^{n} N_i k_i N_i$ can be different, the system stiffness matrix needs to be decomposed to detect individual element damages related to the j^{th} joint. Equations can be solved in different directions. The number of the equations depends on the number of the degree of freedom of the system. Take the model in Figure VIII.2 as an example, in y direction at joint 2, the equation of motion is,

$$\begin{aligned}&\left(N_a k_{a_y} N_a + N_b k_{b_y} N_b + N_c k_{c_y} N_c\right)\left(u_j\right)_y - \left(N_a^* k_{a_y}^* N_a^* + N_b^* k_{b_y}^* N_b^*\right)\left(u_j^*\right)_y \\ &+ N_c^* k_{c_y}^* N_c^* \left(u_j^*\right)_y - m_j \left(\ddot{u}_j\right)_y = m_j^* \left(\ddot{u}_j^*\right)_y\end{aligned} \tag{8.14}$$

$$\beta_1 = \frac{k_{a_y}}{m_j^*} \tag{8.15}$$

$$\beta_2 = \frac{k_{b_y}}{m_j^*} \tag{8.16}$$

$$\beta_3 = \frac{k_{c_y}}{m_j^*} \tag{8.17}$$

$$\beta_4 = \frac{k_{a_y}^*}{m_j^*} \tag{8.18}$$

$$\beta_5 = \frac{k_{b_y}^*}{m_j^*} \tag{8.19}$$

$$\beta_6 = \frac{k_{c_y}^*}{m_j^*} \tag{8.20}$$

$$\beta_{m_j} = \beta_7 \tag{8.21}$$

$$\beta_{k_{a_y}} = \frac{\beta_1}{\beta_4} \tag{8.22}$$

$$\beta_{k_{b_y}} = \frac{\beta_2}{\beta_5} \tag{8.23}$$

$$\beta_{k_{c_y}} = \frac{\beta_3}{\beta_6} \tag{8.24}$$

$$\alpha_{m_j} = \frac{1}{\beta_{m_j}} - 1 \tag{8.25}$$

$$\alpha_{k_{a_y}} = \frac{1}{\beta_{m_{a_y}}} - 1 \tag{8.26}$$

$$\alpha_{k_{b_y}} = \frac{1}{\beta_{k_{b_y}}} - 1 \tag{8.27}$$

$$\alpha_{k_{c_y}} = \frac{1}{\beta_{k_{c_y}}} - 1 \tag{8.28}$$

Eq. (8.15) to Eq. (8.28) present the approach to get the damage indicators at the j^{th} joint. The mass indicators are β_{m_j}, α_{m_j} and stiffness indicators for every member are β_{k_a}, α_{k_a}, β_{k_b}, α_{k_b}, β_{k_c}, α_{k_c}.

Here, the stiffness matrix for each element is,

$$k_i = \begin{bmatrix} \frac{A_i}{L_i} & & \\ & \frac{4I_i}{L_i} & \frac{2I_i}{L_i} \\ & \frac{2I_i}{L_i} & \frac{4I_i}{L_i} \end{bmatrix} E \tag{8.29}$$

When consider different directions, the influence of the damage indicators may be different. For example, for x direction stiffness severity for a certain member, it means the identified damage related to the change of Young's modulus and the sections area. As for y direction, it relates to the changes of Young's modulus and moment of inertia.

8.3 Simulation Procedure for Frame System

In order to validate the presented theory for a frame system, a model has been built in SAP2000, which can be designed into pre-damaged case and post-damaged case. The geometry information of the frame system is shown in Figure VIII.3 and Table VIII.1. The information for cross section properties is shown in Figure VIII.4 The amplitude of the dynamic load applied at joint 2 is 10kips.

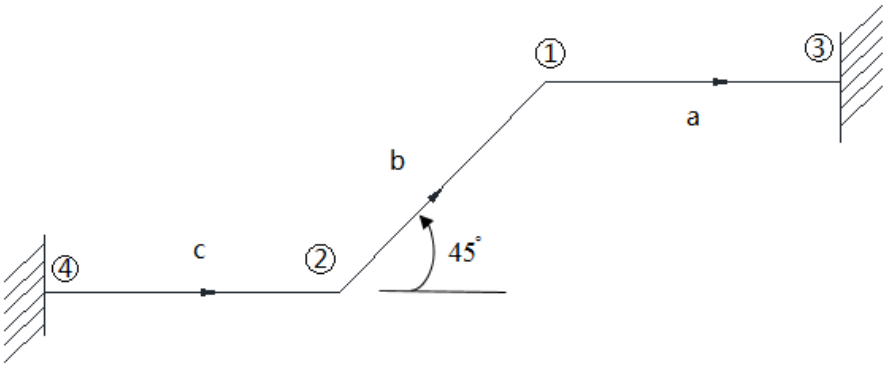

Figure VIII.3 Frame model

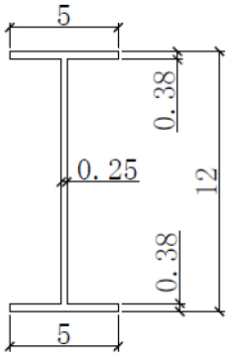

Figure VIII.4 Cross section for frame model

Table VIII.1 The connectivity information of truss model

Frame text	Joint text (left)	Joint text (right)	Length (in)
a	1	3	1
b	2	1	1
c	4	2	1

Table VIII.2 The damage cases for frame system

Case	β_{m_2}	α_{m_2}	β_{k_b}	α_{k_b}	β_{k_c}	α_{k_c}
1	1.11	-0.10	1.00	0.00	1.00	0.00
2	1.00	0.00	1.11	-0.10	1.00	0.00
3	1.11	-0.10	1.11	-0.10	1.00	0.00
4	1.11	-0.10	1.11	-0.10	1.25	-0.20

In this example, four different damage cases are designed. Case 1, Case 2 and Case 3 are focus on single damage location, while Case 4 concerns with multi-damage locations. For Case 1, 2 and 3, the designed damaged element is element b. For Case 4, the damaged elements are element b and element c. The implement of the mass damage is by changing the unit mass volume of the element. The reduction of the stiffness is by changing the value of Young's Modulus of the cross section. Notes that the value of mass at each joint indicates the one at the linked point cross section. Therefore, the change of the mass parameter will indicate the composite results for the related elements. The expected damage indices and damage severities results for each case can be shown in Table VII.4.

8.4 Results for Frame System

The study for the truss system mainly focus on the 2^{nd} joint of the frame model in Table VII.2. The related detection elements are element b, element c. The designed

dynamic load $P_2(t)$ goes horizontally. Therefore, the changes in stiffness damaged indices and stiffness damage severities will mainly focus on element b and element c.

Table VIII.3 Results of damage indicators parameter for beam system

Case	$\beta_{m_2} = m_2 / m_2^*$		$\beta_{k_{b_y}} = k_{b_y} / \mathrm{k}_{b_y}^*$		$\beta_{k_{c_y}} = k_{c_y} / k_{c_y}^*$	
	Calc. Value	Percent Error	Calc. Value	Percent Error	Calc. Value	Percent Error
1	1.11	4.76E-01	1.00	-9.00E-02	1.00	2.34E-03
2	1.00	2.12E-03	1.11	-1.45E-03	1.00	-2.30E-01
3	1.11	8.97E-02	1.11	3.22E-03	1.00	-1.87E-07
4	1.25	-4.41E-04	1.11	1.94E-03	1.25	4.77E-04

Table VIII.4 Results for damage severities for beam system

Case	$\alpha_{m_2} = 1/\beta_{m_2} - 1$		$\alpha_{k_{b_y}} = 1/\beta_{k_{b_y}} - 1$		$\alpha_{k_{c_y}} = 1/\beta_{k_{c_y}} - 1$	
	Calc. Value	Percent Error	Calc. Value	Percent Error	Calc. Value	Percent Error
1	-0.10	9.01E-04	0.00	9.89E-02	1.00	2.33E-03
2	0.00	2.12E-03	-0.10	9.79E-02	1.00	2.99E-01
3	-0.10	1.66E-01	-0.10	1.02E-01	1.00	1.91E-02
4	-0.20	2.00E-01	-0.10	1.01E-01	-0.20	2.00E-01

As mentioned before, the changes of the joint mass indicates the changes to related elements. In other words, the reduction of mass in one element will be expressed

as the change versus the composite value for all related elements. Additionally, the mainly concerned direction for this example is y direction.

By doing dynamic analysis for joint 2, the time-series based acceleration, displacement can be calculated by SAP2000. Using these data to solve Eq. (8.14), the damage indices and damage severities will be calculated to determine the state of the structures, which can be seen in Table VII.3 and Table VII.4.

In Table VII.3, the damage indices have been calculated for each case. In Case 1, the reduction of the parameter is mass at joint 2. In Case 2, the reduction of the stiffness in element b is 10 %. Case 3 is the combination case of Case 1 and Case 2. As for Case 4, it indicates the potential damage locations are element b and element c. In Table VII.4, it is clear to see the calculated damage severities in each case to predict the state of the structures. However, the severities of mass for each case can only indicates the changes at the joint cross section. In other words, the results cannot provide the changes of the mass in each element.

8.5 Conclusion for Frame System

In this Chapter, the application of dynamic ISR in frame system has been introduced. The Node method has been applied to find equation of motion of frame system (Spillers, 1972). Based on the general approach, the frame model has been designed into two cases. One is initial case and the other is final case. By doing dynamic analysis at a certain joint and decomposition of the stiffness matrix, one can calculate the mass indicators at the concerned joints and the damage indicators for each related element.

The results of the simple example for frame system shows great accuracy between the designed and calculated damage indicators. It demonstrates that the dynamic ISR can be used as a Level III method when applied to the frame system, which can not only provide exact damage locations but also damage severities.

As mentioned in Section 7.5, the advantage for the node method is that it can apply dynamic loads at the joints of the frame model. And by using node method it can detect several related elements at the same time. It will definitely save time to find the potential damage regions.

Compared with the truss system, the application of dynamic ISR is more complicated. In order to get the damage indices for every different element, decomposition of the stiffness matrix is necessary. Additionally, the geometry information of the frame system is required.

The concerned direction of the system will impact the results. If the damage of the stiffness occurs in x direction, the reason for the damage may be the reduction of the Young's Modulus or the change of the cross section area. If the stiffness happens in y direction, it means the damage comes from the change of Young's Modulus or the moment of inertia. Moreover, the change of the mass can be shown as the composite results of every related member. The detailed damage severities for every related element cannot be provided by this method. However, this problem can be solved by comprehensively using the general approach of beam system and node method. One can use node method to find a potential mass damage joint. Then using general beam FEM approach for each potential element to get the detailed mass damage information.

CHAPTER IX

CONCLUSION AND FUTURE WORK

9.1 Conclusions

The goal of this research is to propose an effective Level III NDE method to detect the existence, location and severity of damage in structures. The proposed method is called dynamic ISR method. The essential principle of this theory is the net internal force at any given section is not impact by the inflicted damage. Therefore, this method potentially can be applied to nearly all types of structures.

In the first two chapters, an introduction and a literature review of vibration based NDE method have been provided. From Chapter III to Chapter VIII, the definition of dynamic ISR method has been applied to different types of structures, which includes discrete-parameter system, rod system, beam system, truss system and frame system. And the simulation procedures for special type of structures are mainly divided into four steps:

1) General review of the system.

2) Application of the dynamic ISR theory for the system.

3) Simulation procedures for the concerned system.

4) Results and conclusion for the special system.

The research also provide general approaches for different type of structures based on finite element method. By analyzing the free-body diagram of the unit member, set up equations by the invariant stress resultants at a certain cross section for initial and

final system. Based on the data calculated by SAP 2000 to solve for damage indices and damage severities for the structures, which can help to locate and characterize damages.

Based on the results for different types of structures, the proposed dynamic ISR method can provide clear indicators to accurately locate and characterize multiple damage locations. The detected damages can be mass, damping and stiffness damages from nearly all type of structures. Additionally, it is sensitive to detect small and inaccessible damage. No analytical model of the structure is required and only experimental data is needed to complete the analyses. The computational process is based on vibration theory, which is straight-forward and robust.

9.2 Future Work

As presented in the thesis, the dynamic ISR method is an explicit damage identification method which can be applied into different types of structures. Future research can be focus on:

- Application in Timoshenko beam system
- Damping damage detection in beam system
- Application to 3-D examples, such as plate structures and shell structures.
- Field data is needed to verify the accuracy of this method

REFERENCES

Adams, R. D., Cawley, P., Pye, C. J., and Stone, B. J. (1978). "A vibration technique for non-destructively assessing the integrity of structures." *Journal of Mechanical Engineering Science*, 20(2), 93-100.

Allemang, R. J., and Brown, D. L. (1982). "A correlation coefficient for modal vector analysis." *In Proceedings of the 1st International Modal Analysis Conference* (Vol. 1, pp. 110-116). SEM, Orlando, FL.

Aktan, A. E., Lee, K. L., Chuntavan, C., and Aksel, T. (1994). "Modal testing for structural identification and condition assessment of constructed facilities." *In Proceedings of the 12th International Modal Analysis Conference*. SPIE INTERNATIONAL SOCIETY FOR OPTICAL, 462-468.

Catbas, F. N., Gul, M., and Burkett, J. L. (2008). "Conceptual damage-sensitive features for structural health monitoring: laboratory and field demonstrations." *Mechanical Systems and Signal Processing*, 22(7), 1650-1669.

Cawley, P., and Adams, R. D. (1979). "The location of defects in structures from measurements of natural frequencies." *Journal of Strain Analysis for Engineering Design*, 14(2), 49-57.

Chance, J., Tomlinson, G. R., and Worden, K. (1994). "A simplified approach to the numerical and experimental modeling of the dynamics of a cracked beam." *In Proceedings of the 12th International Modal Analysis Conference*, 778-785. SPIE INTERNATIONAL SOCIETY FOR OPTICAL

Dincal, S., and N. Stubbs. (2013). "Damage evaluation of Timoshenko beams using invariant stress resultants." *Engineering Structures* 56 (2013): 2052-2064.

Doebling, S. W. (1996). "Minimum-rank optimal update of elemental stiffness parameters for structural damage identification." *AIAA* 1. 34(12), 2615-2621.

Doebling, S. W., Farrar, C. R, Prime, M. B., and Shevitz, D. W. (1996). "Damage identification and health monitoring of structural and mechanical systems from

changes in their vibration characteristics: A literature review." *Los Alamos National Laboratory Report* LA-13070-MS, CA.

Doebling, S. W., Peterson, L. D., and Alvin, K. F. (1996). "Estimation of reciprocal residual flexibility from experimental modal data." *AIAA Journal*, 34(8), 1678-1685.

Farrar, C. R., and Jauregui, D. Y. (1996). "Damage detection algorithms applied to experimental and numerical modal data from the 1-40 bridge*." Los Alamos National Laboratory Report* LA-13074-MS, CA.

Farrar, C. R., and Worden, K. (2007). "An introduction to structural health monitoring. Philosophical Transactions of the Royal Society A: Mathematical." *Physical and Engineering Sciences*, 365(1851), 303-315.

Federal Highway Administration. (2007). "Chapter 6 - Evaluation of LS-DYNA Concrete Mate." *FHWA-HRT*, 05-063

Friswell, M. I., Penny, J.E.T., and Wilson, D.A.L. (1994). "Using vibration data and statistical measures to locate damage in structures." *Modal Analysis: The International Journal of Analytical and Experimental Modal Analysis* 9(4), 239-254..

Li, R. (2013). "Non-destructive evaluation based on element strain energy." Thesis, Texas A&M University, College Station, TX.

Lieven, N. A. J., and Ewins, D. J. (1988, February). "Spatial correlation of mode shapes, the coordinate modal assurance criterion (COMAC)." *In Proceedings of the Sixth International Modal Analysis Conference* (Vol. 1, pp. 690-695). Kissimmee., FL.

Juneja, V., Haftka, R. T., and Cudney, H. H. (1997). "Damage detection and damage detectability-analysis and experiments." *Journal of Aerospace Engineering*, 10(4), 135-142.

Mayes, R. L. (1992). "Error localization using mode shapes-An application to a two link robot arrn." *In Proceedings of the 10th International Modal Analysis Conference*, 886-891. Albuquerque, NM.

Mayes, R. L. (1995). "An experimental algorithm for detecting damage applied to the 1-40 bridge over the Rio Grande." *Smart Structures and Materials*, 204-214.

Pandey, A. K., Biswas, M., and Samman, M. M. (1991). "Damage detection from changes in curvature mode shapes." *Journal of Sound and Vibration*.145 (2), 321-332.

Pandey, A. K., and Biswas, M. (1994). "Damage detection in structures using changes in flexibility." *Journal of Sound and Vibration*, 169(1), 3-17.

Pandey, A. K., and Biswas, M. (1995). "Damage diagnosis of truss structures by estimation of flexibility change." *Modal Analysis: The International Journal of Analytical and Experimental Modal Analysis* 10(2), 104-117.

Peterson, L. D., Alvin, K. F., Doebling, S. W., and Park, K. C. (1993). "Damage detection using experimentally measured mass and stiffness matrices." *In Proceedings of the 34th AIAAIASMElASCElAHSIASC Structures, Structural Dynamics, and Materials Conference, AIAA-93-1482-CP*, 1518-1528, LA, Jolla, CA.

Peterson, L. D., Doebling, S. W., and Alvin, K. F. (1995). "Experimental determination of local structural stiffness by disassembly of measured flexibility matrices." *In Proceedings of the 36th A1AA1ASMEIASCEI AHSIASC Structures, Structural Dynamics, and Materials Conference, AIAA-95-1090-CP*, 2756-2766, New Orleans, LA.

Ratcliffe, C. P. (1997). "Damage detection using a modified Laplacian operator on mode shape data." *Journal of Sound and Vibration*. 204(3), 505-517.

Rytter, A. (1993). "Vibration based inspection of civil engineering structures." *Ph.D. dissertation*, Aalborg University, Esbjerg Copenhagen, Denmark.

Salawu, O. S. and Williams, C. (1993). "Structural damage detection using experimental modal analysis-A comparison of some methods." *In Proceedings of the 11th International Modal Analysis Conference*, pp. 254-260. SEM SOCIETY FOR EXPERIMENTAL MECHANICS INC

Salawu, O. S. (1997a). “Detection of structural damage through changes in frequency: a review.” *Engineering structures*, 19(9), 718-723.

Salawu, O. S. (1997b). “An integrity index method for structural assessment of engineering structures using modal testing.” *Insight* 39(1), 33-37.

Spillers, W. R. (1972).”Automated structural analysis: an introduction.” *Elsevier*. Columbia University, New York, NY.

Stubbs, N., Broome, T. H., and Osegueda, R. (1990). “Nondestructive construction error detection in large space structures.” *A1AA J*. 28(1), 146152.

Stubbs, N. and Kim, I.-T. (1996). “"Damage localization in structures without baseline modal parameters.” *A1AA J*. 34(8), 1644-1649.

Stubbs, N., Kim, I.-T., and Topole, K. (1992). “An efficient and robust algorithm for damage localization in offshore platforms.” *In Proceedings of the ASCE Tenth Structures Congress*, 543-546. New York, NY.

Stubbs, N., and Osegueda, R. (1990). “Global non-destructive damage evaluation in solids.” *International Journal of Analytical and Experimental Modal Analysis*, 5, 67-79.

Toksoy, T. and Aktan, A. E. (1994). “Bridge-condition assessment by modal flexibility.” *Exp. Mech*. 34, 271-278.

Vandiver, J. K. (1975). “Detection of structural failure on fixed platforms by measurement of dynamic response.” *In Offshore Technology Conference. Offshore Technology Conference*. Houston, TX.

Whittome, T. R., and Dodds, C. J. (1983). “Monitoring offshore structures by vibration techniques.” *In Proceedings of Design in Offshore Structures Conference*, 93-100. Houston, TX.

Wojnarowski, M. E., Stiansen, S. G., and Reddy, N. E. (1977). "Structural integrity evaluation of a fixed platform using vibration criteria." *In Proceedings of the 9th Annual Offshore Technology Conference*, 247-256. Houston, TX.

Yao, J. T. (1972). "Concept of structural control." *Journal of the Structural Division*, 98(7), 1567-1574.

Zhang, Z., and Atkan, A. E. (1995). "The damage indices for constructed facilities." *In Proceedings of the 13th International Modal Analysis Conference*, 1520-1529. Nashville, TN.

APPENDIX A

Table A.1 Description of damage Case 1 for SDF model

	Mass (kip-s^2)/in	Damping (kip-s/in)	Stiffness (kip/in)	Force Amplitude (kips)
Undamaged	3.00	1.00	2.00	1.00
Damaged	2.40	1.00	2.00	1.00

Table A.2 Results for Case 1 for SDOF model based on same time step number

Time step size	$\beta_m = m/m^*$		$\beta_c = c/c^*$		$\beta_k = k/k^*$	
	Calc. Value	Percent Error	Calc. Value	Percent Error	Calc. Value	Percent Error
5E-03	1.25	6.91E-04	1.00	2.59E-01	1.00	-1.97E-01
1E-02	1.25	-4.38E-05	1.00	8.05E-05	1.00	2.03E-05
2E-02	1.25	-2.62E-08	1.00	-2.00E-05	1.00	1.00E-05
5E-02	1.25	-1.32E-08	1.00	5.93E-06	1.00	-3.10E-06

Notes: Number of the time step for each case is 50.

Table A.3 Results for Case 1 for SDOF model based on same time step size

Time step number	$\beta_m = m/m^*$		$\beta_c = c/c^*$		$\beta_k = k/k^*$	
	Calc. Value	Percent Error	Calc. Value	Percent Error	Calc. Value	Percent Error
5E01	1.25	6.91E-04	1.00	2.59E-01	1.00	-1.97E-02
1E02	1.25	-1.23E-05	1.00	1.30E-03	1.00	-8.00E-04

Notes: Output time step size 0.005.

Table A.4 Description of damage case 2 for SDOF model

	Mass (kip-s^2)/in	Damping (kip-s/in)	Stiffness (kip/in)	Force Amplitude (kips)
Undamaged	3.00	1.00	2.00	1.00
Damaged	2.40	0.90	2.00	1.00

Table A.5 Results for case 2 for SDOF model based on same time step number

Time step size	$\beta_m = m/m^*$		$\beta_c = c/c^*$		$\beta_k = k/k^*$	
	Calc. Value	Percent Error	Calc. Value	Percent Error	Calc. Value	Percent Error
5E-03	1.00	-4.66E-03	1.08	2.45E00	1.00	-4.63E-01
1E-02	1.00	7.00E-04	1.11	-6.09E-02	1.00	8.47E-03
2E-02	1.00	1.88E-06	1.11	-1.03E-02	1.00	5.94E-05
5E-02	1.00	-1.40E-08	1.11	-1.00E-03	1.00	-2.7E-06

Notes: Number of the time step for each case is 50.

Table A.6 Results for case 2 for SDOF model based on same time step size

Time step number	$\beta_m = m/m^*$		$\beta_c = c/c^*$		$\beta_k = k/k^*$	
	Calc. Value	Percent Error	Calc. Value	Percent Error	Calc. Value	Percent Error
5E01	1.00	-4.66E-03	1.08	2.45E00	1.00	-4.63E-02
1E02	1.00	1.05E-03	1.11	9.21E-02	1.00	-1.59E-02

Notes: Output time step size 0.005

Table A.7 Description of damage case 3 for SDOF model

	Mass (kip-s^2)/in	Damping (kip-s/in)	Stiffness (kip/in)	Force Amplitude (kips)
Undamaged	3.00	1.00	2.00	1.00
Damaged	3.00	1.00	1.40	1.00

TableA.8 Results for case 3 for SDOF model based on same time step number

Time step size	$\beta_m = m/m^*$		$\beta_c = c/c^*$		$\beta_k = k/k^*$	
	Calc. Value	Percent Error	Calc. Value	Percent Error	Calc. Value	Percent Error
5E-03	1.00	4.91E-03	1.00	7.19E-04	1.42	6.39E-01
1E-02	1.00	1.16E-04	1.00	4.38E-05	1.43	-4.08E-03
2E-02	1.00	1.33E-07	1.00	1.28E-07	1.43	-1.20E-04
5E-02	1.00	-7.6E-09	1.00	9.3E-08	1.43	-1.00E-04

Notes: Number of the time step for each case is 50.

Table A.9 Results for case 3 for SDOF model based on same time step size

Time step number	$\beta_m = m/m^*$		$\beta_c = c/c^*$		$\beta_k = k/k^*$	
	Calc. Value	Percent Error	Calc. Value	Percent Error	Calc. Value	Percent Error
5E01	1.00	4.91E-03	1.00	7.19E-03	1.43	6.39E-01
1E02	1.00	9.52E-05	1.00	-1.3E-04	1.43	-7.35E-02

Notes: Output time step size 0.005

Table A.10 Description of damage case 4 for SDOF model

	Mass (kip-s^2)/in	Damping (kip-s/in)	Stiffness (kip/in)	Force Amplitude (kips)
Undamaged	3.00	1.00	2.00	1.00
Damaged	2.40	0.90	2.00	1.00

Table A.11 Results for case 4 for SDOF model based on same time step number

Time step size	$\beta_m = m/m^*$		$\beta_c = c/c^*$		$\beta_k = k/k^*$	
	Calc. Value	Percent Error	Calc. Value	Percent Error	Calc. Value	Percent Error
5E-03	1.25	-2.41E-03	1.11	3.69E-03	1.00	-2.98E-02
1E-02	1.25	3.04E-05	1.11	-9.71E-03	1.00	-6.2E-03
2E-02	1.25	3.76E-09	1.11	1.00E-02	1.00	1.46E-05
5E-02	1.25	-1.5E-08	1.11	-1.00E-02	1.00	-3.00E-06

Notes: Number of the time step for each case is 50.

Table A.12 Results for case 4 for SDOF model based on same time step size

Time step number	$\beta_m = m/m^*$		$\beta_c = c/c^*$		$\beta_k = k/k^*$	
	Calc. Value	Percent Error	Calc. Value	Percent Error	Calc. Value	Percent Error
5E01	1.25	-2.40E-03	1.11	3.69E-03	1.00	-2.98E-02
1E02	1.25	-3.20E-05	1.11	-1.03E-02	1.00	5.00E-04

Notes: Output time step size 0.005

Table A.13 Description of damage case 5 for SDOF model

	Mass (kip-s^2)/in	Damping (kip-s/in)	Stiffness (kip/in)	Force Amplitude (kips)
Undamaged	3.00	1.00	2.00	1.00
Damaged	2.40	1.00	1.40	1.00

Table A.14 Results for case 5 for SDOF model based on same time step number

Time step size	$\beta_m = m/m^*$		$\beta_c = c/c^*$		$\beta_k = k/k^*$	
	Calc. Value	Percent Error	Calc. Value	Percent Error	Calc. Value	Percent Error
5E-03	1.25	-9.60E-03	1.00	4.76E-01	1.43	-3.91E-01
1E-02	1.25	8.27E-05	1.00	-2.88E-03	1.43	-2.90E-03
2E-02	1.25	1.03E-06	1.00	5.4E-06	1.43	-1.00E-04
5E-02	1.25	-2.00E-08	1.00	2.45E-06	1.43	-1.00E-04

Notes: Number of the time step for each case is 50.

Table A.15 Results for case 5 for SDOF model based on same time step size

Time step number	$\beta_m = m/m^*$		$\beta_c = c/c^*$		$\beta_k = k/k^*$	
	Calc. Value	Percent Error	Calc. Value	Percent Error	Calc. Value	Percent Error
5E01	1.25	-9.57E-03	1.00	4.76E-01	1.43	-3.91E-03
1E02	1.25	1.94E-04	1.00	7.47E-04	1.43	-8.50E-04

Notes: Output time step size 0.005

Table A.16 Description of damage case 6 for SDOF model

	Mass (kip-s^2)/in	Damping (kip-s/in)	Stiffness (kip/in)	Force Amplitude (kips)
Undamaged	3.00	1.00	2.00	1.00
Damaged	3.00	0.90	1.40	1.00

Table A.17 Results for case 6 for SDOF model based on same time step number

Time step size	$\beta_m = m/m^*$		$\beta_c = c/c^*$		$\beta_k = k/k^*$	
	Calc. Value	Percent Error	Calc. Value	Percent Error	Calc. Value	Percent Error
5E-03	1.00	-9.60E-03	1.11	-5.55E-01	1.00	-2.98E-00
1E-02	1.00	8.27E-05	1.11	-8.55E-03	1.00	-6.04E-03
2E-02	1.00	1.03E-06	1.11	9.99E-03	1.00	-1.20E-04
5E-02	1.00	-2.00E-08	1.11	-1.00E-02	1.00	-1.10E-04

Notes: Number of the time step for each case is 50.

Table A.18 Results for case 6 for SDOF model based on same time step size

Time step number	$\beta_m = m/m^*$		$\beta_c = c/c^*$		$\beta_k = k/k^*$	
	Calc. Value	Percent Error	Calc. Value	Percent Error	Calc. Value	Percent Error
5E01	1.00	-1.10E-03	1.11	-5.55E-01	1.39	2.98E00
1E02	1.00	-3.30E-05	1.11	-1.08E-02	1.43	-8.50E-04

Notes: Output time step size 0.005

Table A.19 Description of damage case 7 for SDOF model

	Mass (kip-s^2)/in	Damping (kips-s/in)	Stiffness (kip/in)	Force Amplitude (kips)
Undamaged	3.00	1.00	2.00	1.00
Damaged	2.40	0.90	1.40	1.00

Table A.20 Results for case 7 for SDOF model based on same time step number

Time step size	$\beta_m = m/m^*$		$\beta_c = c/c^*$		$\beta_k = k/k^*$	
	Calc. Value	Percent Error	Calc. Value	Percent Error	Calc. Value	Percent Error
5E-03	1.25	-4.21E-03	1.12	-1.15E00	1.40	2.41E-00
1E-02	1.25	1.37E-04	1.11	-3.10E-03	1.43	-1.57E-02
2E-02	1.25	3.80E-07	1.11	9.99E-04	1.43	-1.60E-05
5E-02	1.25	-4.97E-09	1.11	-1.00E-03	1.43	-6.10E-06

Notes: Number of the time step for each case is 50.

Table A.21 Results for case 7 for SDOF model based on same time step size

Time step number	$\beta_m = m/m^*$		$\beta_c = c/c^*$		$\beta_k = k/k^*$	
	Calc. Value	Percent Error	Calc. Value	Percent Error	Calc. Value	Percent Error
5E01	1.25	4.21E-03	1.12	-1.15E00	1.39	2.41E00
1E02	1.25	3.20E-04	1.11	-9.00E-03	1.43	-3.2E-03

Notes: Output time step size 0.005.

Table A.22 Results for Case 1 for rod system

Element Number	$\beta_m = m / m^*$			$\beta_k = k / k^*$		
	Calculated	Actual	Percent Error	Calculated	Actual	Percent Error
1	1.00	1.00	-1.96E-02	1.00	1.00	6.09E-04
2	1.00	1.00	-6.53E-03	1.00	1.00	1.87E-04
3	1.00	1.00	1.96E-02	1.00	1.00	-1.66E-04
4	1.00	1.00	1.70E-02	1.00	1.00	2.56E-04
5	1.00	1.00	-1.20E-02	1.00	1.00	5.87E-06
6	1.00	1.00	-1.67E-03	1.00	1.00	-4.09E-05
7	1.00	1.00	4.43E-03	1.00	1.00	-3.43E-04
8	1.00	1.00	1.43E-03	1.00	1.00	1.71E-04
9	1.00	1.00	-9.89E-03	1.00	1.00	-2.93E-05
10	1.00	1.00	7.36E-03	1.00	1.00	-1.00E-04
11	1.00	1.00	3.84E-03	1.00	1.00	2.18E-04
12	1.00	1.00	1.51E-03	1.00	1.00	7.30E-04
13	1.00	1.00	-2.89E-03	1.00	1.00	9.53E-04
14	1.00	1.00	7.69E-04	1.00	1.00	1.46E-04
15	1.00	1.00	-1.72E-03	1.00	1.00	2.92E-04
16	1.00	1.00	-7.19E-04	1.00	1.00	-1.04E-04

Table A.22 Results for Case 1 for rod system (continued)

Element Number	$\beta_m = m/m^*$			$\beta_k = k/k^*$		
	Calculated	Actual	Percent Error	Calculated	Actual	Percent Error
17	1.11	1.11	3.09E-03	1.00	1.00	6.09E-04
18	1.00	1.00	-2.40E-03	1.00	1.00	1.87E-04
19	1.00	1.00	-3.99E-03	1.00	1.00	-1.66E-04
20	1.00	1.00	-1.07E-03	1.00	1.00	2.56E-04
21	1.00	1.00	-1.62E-04	1.00	1.00	5.87E-06
22	1.00	1.00	2.44E-02	1.00	1.00	-4.09E-05
23	1.00	1.00	4.45E-04	1.00	1.00	-3.43E-04
24	1.00	1.00	-1.22E-03	1.00	1.00	1.71E-04
25	1.00	1.00	-1.27E-03	1.00	1.00	-2.93E-05
26	1.00	1.00	-1.59E-03	1.00	1.00	-1.00E-04
27	1.00	1.00	8.30E-04	1.00	1.00	2.18E-04
28	1.00	1.00	2.57E-03	1.00	1.00	7.30E-04
29	1.00	1.00	6.66E-04	1.00	1.00	9.53E-04
30	1.00	1.00	1.34E-03	1.00	1.00	1.46E-04

Table A.23 Results for Case 2 for rod system

Element Number	$\beta_m = m / m^*$			$\beta_k = k / k^*$		
	Calculated	Actual	Percent Error	Calculated	Actual	Percent Error
1	1.00	1.00	1.14E-02	1.00	1.00	2.24E-04
2	1.00	1.00	-4.32E-02	1.00	1.00	-1.10E-04
3	1.00	1.00	-8.11E-04	1.00	1.00	-1.29E-04
4	1.00	1.00	3.11E-03	1.00	1.00	2.61E-04
5	1.00	1.00	-1.09E-02	1.00	1.00	1.15E-04
6	1.00	1.00	1.58E-03	1.00	1.00	3.46E-03
7	1.00	1.00	-2.54E-03	1.00	1.00	-6.40E-05
8	1.00	1.00	2.78E-03	1.00	1.00	-2.67E-04
9	1.00	1.00	-6.37E-03	1.00	1.00	-8.13E-05
10	1.00	1.00	6.77E-04	1.00	1.00	1.28E-03
11	1.00	1.00	-2.42E-04	1.00	1.00	4.64E-05
12	1.00	1.00	-1.02E-04	1.00	1.00	3.08E-04
13	1.00	1.00	-2.40E-03	1.00	1.00	8.39E-04
14	1.00	1.00	1.32E-03	1.00	1.00	1.88E-04
15	1.00	1.00	-1.78E-03	1.00	1.00	2.09E-04
16	1.00	1.00	-3.05E-03	1.00	1.00	1.29E-04

Table A.23 Results for Case 2 for rod system (continued)

Element Number	$\beta_m = m / m^*$			$\beta_k = k / k^*$		
	Calculated	Actual	Percent Error	Calculated	Actual	Percent Error
17	1.00	1.00	6.67E-04	1.18	1.18	-3.37E-04
18	1.00	1.00	-3.63E-03	1.00	1.00	4.94E-04
19	1.00	1.00	-1.81E-03	1.00	1.00	-6.66E-05
20	1.00	1.00	2.05E-03	1.00	1.00	3.62E-04
21	1.00	1.00	9.65E-06	1.00	1.00	3.21E-04
22	1.00	1.00	3.72E-03	1.00	1.00	-3.66E-05
23	1.00	1.00	1.38E-03	1.00	1.00	-2.09E-04
24	1.00	1.00	-4.90E-04	1.00	1.00	1.82E-04
25	1.00	1.00	-1.97E-03	1.00	1.00	-1.00E-04
26	1.00	1.00	3.66E-04	1.00	1.00	-1.01E-04
27	1.00	1.00	2.77E-04	1.00	1.00	3.74E-05
28	1.00	1.00	5.94E-04	1.00	1.00	2.38E-04
29	1.00	1.00	2.75E-04	1.00	1.00	2.29E-04
30	1.00	1.00	3.16E-03	1.00	1.00	8.08E-05

Table A.24 Results for Case 3 for rod system

Element Number	$\beta_m = m / m^*$			$\beta_k = k / k^*$		
	Calculated	Actual	Percent Error	Calculated	Actual	Percent Error
1	1.00	1.00	-6.36E-02	1.00	1.00	5.01E-04
2	1.00	1.00	1.01E-02	1.00	1.00	4.64E-04
3	1.00	1.00	2.24E-03	1.00	1.00	1.18E-04
4	1.00	1.00	8.77E-03	1.00	1.00	2.27E-04
5	1.00	1.00	9.48E-04	1.00	1.00	7.96E-05
6	1.00	1.00	6.18E-03	1.00	1.00	1.47E-04
7	1.00	1.00	3.75E-03	1.00	1.00	-9.56E-05
8	1.00	1.00	-7.88E-04	1.00	1.00	1.41E-04
9	1.00	1.00	-1.00E-02	1.00	1.00	5.46E-06
10	1.00	1.00	-2.86E-03	1.00	1.00	5.93E-05
11	1.00	1.00	-1.74E-03	1.00	1.00	7.07E-05
12	1.00	1.00	1.53E-02	1.00	1.00	3.58E-04
13	1.00	1.00	-1.41E-04	1.00	1.00	9.35E-04
14	1.00	1.00	5.13E-03	1.00	1.00	4.69E-04
15	1.00	1.00	5.18E-04	1.00	1.00	1.61E-04
16	1.00	1.00	2.21E-03	1.00	1.00	1.09E-04

Table A.24 Results for Case 3 for rod system (continued)

Element Number	$\beta_m = m / m^*$			$\beta_k = k / k^*$		
	Calculated	Actual	Percent Error	Calculated	Actual	Percent Error
17	1.11	1.11	-7.65E-03	1.18	1.18	-1.28E-05
18	1.00	1.00	8.67E-04	1.00	1.00	5.45E-04
19	1.00	1.00	-2.87E-04	1.00	1.00	-1.02E-04
20	1.00	1.00	9.26E-04	1.00	1.00	3.65E-04
21	1.00	1.00	-5.97E-04	1.00	1.00	2.97E-04
22	1.00	1.00	4.64E-04	1.00	1.00	-6.06E-04
23	1.00	1.00	3.12E-03	1.00	1.00	-2.04E-04
24	1.00	1.00	-2.43E-03	1.00	1.00	2.89E-04
25	1.00	1.00	1.04E-04	1.00	1.00	-4.42E-04
26	1.00	1.00	-1.41E-03	1.00	1.00	-1.87E-04
27	1.00	1.00	3.14E-03	1.00	1.00	-4.51E-05
28	1.00	1.00	1.11E-03	1.00	1.00	1.62E-04
29	1.00	1.00	-1.65E-03	1.00	1.00	1.60E-06
30	1.00	1.00	1.21E-03	1.00	1.00	2.84E-05

Table A.25 Results for Case 4 for rod system

Element Number	$\beta_m = m / m^*$			$\beta_k = k / k^*$		
	Calculated	Actual	Percent Error	Calculated	Actual	Percent Error
1	1.00	1.00	3.26E-02	1.00	1.00	3.24E-04
2	1.00	1.00	-2.91E-02	1.00	1.00	5.50E-04
3	1.00	1.00	-8.01E-04	1.00	1.00	4.47E-04
4	1.00	1.00	1.45E-02	1.00	1.00	-5.23E-05
5	1.00	1.00	-4.73E-03	1.00	1.00	2.65E-04
6	1.00	1.00	3.24E-03	1.00	1.00	1.43E-04
7	1.00	1.00	1.67E-03	1.00	1.00	-3.47E-04
8	1.00	1.00	-3.40E-04	1.00	1.00	-1.09E-04
9	1.00	1.00	-4.59E-04	1.00	1.00	-1.28E-04
10	1.00	1.00	-1.34E-03	1.00	1.00	-2.64E-04
11	1.00	1.00	-3.87E-03	1.00	1.00	3.82E-04
12	1.00	1.00	1.56E-03	1.00	1.00	2.11E-04
13	1.00	1.00	3.75E-05	1.00	1.00	8.35E-04
14	1.00	1.00	3.19E-03	1.00	1.00	4.28E-04
15	1.00	1.00	2.68E-03	1.00	1.00	3.90E-05
16	1.00	1.00	2.37E-03	1.00	1.00	-5.66E-04

Table A.25 Results for Case 4 for rod system (continued)

Element Number	$\beta_m = m / m^*$			$\beta_k = k / k^*$		
	Calculated	Actual	Percent Error	Calculated	Actual	Percent Error
17	1.11	1.11	2.69E-03	1.18	1.18	-3.57E-04
18	1.00	1.00	-1.31E-03	1.00	1.00	1.39E-04
19	1.00	1.00	-2.49E-03	1.00	1.00	-4.65E-04
20	1.00	1.00	-1.47E-03	1.00	1.00	2.81E-04
21	1.00	1.00	-2.70E-04	1.00	1.00	1.83E-04
22	1.00	1.00	5.29E-04	1.00	1.00	-1.72E-04
23	1.00	1.00	3.16E-04	1.00	1.00	-4.63E-04
24	1.00	1.00	4.53E-04	1.00	1.00	-2.17E-04
25	1.00	1.00	4.2-E-04	1.00	1.00	-3.96E-04
26	1.00	1.00	5.60E-04	1.00	1.00	-2.39E-04
27	1.25	1.25	3.65E-04	1.22	1.22	1.20E-04
28	1.00	1.00	1.52E-04	1.00	1.00	3.48E-04
29	1.00	1.00	2.16E-04	1.00	1.00	1.05E-04
30	1.00	1.00	1.45E-04	1.00	1.00	-1.59E-04

Table A.26 Results for Case 1 for simply supported beam system

Element Number	$\beta_m = m / m^*$			$\beta_k = k / k^*$		
	Calculated	Actual	Percent Error	Calculated	Actual	Percent Error
1	1.00	1.00	6.99E-03	1.00	1.00	2.09E-04
2	1.00	1.00	4.14E-03	1.00	1.00	1.03E-04
3	1.00	1.00	6.33E-04	1.00	1.00	1.34E-05
4	1.00	1.00	4.27E-03	1.00	1.00	5.28E-05
5	1.00	1.00	1.63E-03	1.00	1.00	1.2E-05
6	1.00	1.00	4.44E-03	1.00	1.00	3.33E-05
7	1.00	1.00	3.63E-03	1.00	1.00	2.41E-05
8	1.00	1.00	2.45E-03	1.00	1.00	1.91E-05
9	1.00	1.00	5.37E-03	1.00	1.00	3.03E-05
10	1.00	1.00	2.25E-04	1.00	1.00	5.39E-06
11	1.00	1.00	7.06E-03	1.00	1.00	3.50E-05
12	1.00	1.00	3.21E-03	1.00	1.00	8.58E-06
13	1.00	1.00	7.01E-03	1.00	1.00	3.78E-05
14	1.00	1.00	8.83E-03	1.00	1.00	2.50E-05
15	1.00	1.00	8.72E-03	1.00	1.00	4.86E-05
16	1.00	1.00	4.73E-03	1.00	1.00	4.02E-05

Table A.22 Results for Case 1 for simply supported beam system (continued)

Element Number	$\beta_m = m / m^*$			$\beta_k = k / k^*$		
	Calculated	Actual	Percent Error	Calculated	Actual	Percent Error
17	1.11	1.11	7.04E-03	1.00	1.00	9.78E-05
18	1.00	1.00	6.33E-04	1.00	1.00	2.66E-05
19	1.00	1.00	2.26E-03	1.00	1.00	4.62E-05
20	1.00	1.00	3.72E-02	1.00	1.00	1.51E-05
21	1.00	1.00	3.55E-02	1.00	1.00	3.01E-05
22	1.00	1.00	2.78E-02	1.00	1.00	3.53E-06
23	1.00	1.00	2.63E-02	1.00	1.00	2.34E-05
24	1.00	1.00	3.03E-02	1.00	1.00	3.32E-06
25	1.00	1.00	3.32E-02	1.00	1.00	1.98E-05
26	1.00	1.00	3.06E-02	1.00	1.00	8.44E-06
27	1.00	1.00	2.80E-02	1.00	1.00	1.96E-05
28	1.00	1.00	2.91E-02	1.00	1.00	1.64E-05
29	1.00	1.00	3.16E-02	1.00	1.00	2.81E-05
30	1.00	1.00	3.33E-02	1.00	1.00	6.97E-05

Table A.27 Results for Case 2 for simply supported beam system

Element Number	$\beta_m = m / m^*$			$\beta_k = k / k^*$		
	Calculated	Actual	Percent Error	Calculated	Actual	Percent Error
1	1.00	1.00	-1.56E-01	1.00	1.00	-4.60E-03
2	1.00	1.00	-9.72E-02	1.00	1.00	-2.50E-03
3	1.00	1.00	5.20E-03	1.00	1.00	1.34E-04
4	1.00	1.00	9.36E-02	1.00	1.00	1.32E-03
5	1.00	1.00	5.58E-02	1.00	1.00	5.21E-04
6	1.00	1.00	-7.85E-02	1.00	1.00	-6.60E-04
7	1.00	1.00	-9.35E-02	1.00	1.00	-6.90E-04
8	1.00	1.00	1.78E-02	1.00	1.00	1.86E-04
9	1.00	1.00	1.07E-01	1.00	1.00	7.34E-04
10	1.00	1.00	4.72E-02	1.00	1.00	2.76E-04
11	1.00	1.00	-9.34E-02	1.00	1.00	-4.80E-04
12	1.00	1.00	-9.92E-02	1.00	1.00	-5.60E-04
13	1.00	1.00	3.30E-02	1.00	1.00	1.77E-04
14	1.00	1.00	1.28E-01	1.00	1.00	6.76E-04
15	1.00	1.00	4.75E-02	1.00	1.00	1.27E-04
16	1.00	1.00	-1.07E-01	1.00	1.00	-7.00E-04

Table A.23 Results for Case 2 for simply supported beam system (continued)

Element Number	$\beta_m = m / m^*$			$\beta_k = k / k^*$		
	Calculated	Actual	Percent Error	Calculated	Actual	Percent Error
17	1.00	1.00	-4.75E-02	1.18	1.18	-8.70E-04
18	1.00	1.00	-2.08E-02	1.00	1.00	-5.40E-04
19	1.00	1.00	2.54E-02	1.00	1.00	-4.70E-04
20	1.00	1.00	6.04E-02	1.00	1.00	2.66E-04
21	1.00	1.00	1.27E-02	1.00	1.00	1.16E-04
22	1.00	1.00	-4.12E-02	1.00	1.00	-2.30E-04
23	1.00	1.00	-2.68E-02	1.00	1.00	-1.70E-04
24	1.00	1.00	2.47E-02	1.00	1.00	1.97E-04
25	1.00	1.00	4.00E-02	1.00	1.00	3.44E-04
26	1.00	1.00	-7.75E-03	1.00	1.00	2.65E-6
27	1.00	1.00	-3.48E-02	1.00	1.00	-2.50E-04
28	1.00	1.00	-7.62E-03	1.00	1.00	-8.20E-05
29	1.00	1.00	3.24E-02	1.00	1.00	8.41E-04
30	1.00	1.00	5.71E-02	1.00	1.00	1.81E-03

Table A.28 Results for Case 3 for simply supported beam system

Element Number	$\beta_m = m / m^*$			$\beta_k = k / k^*$		
	Calculated	Actual	Percent Error	Calculated	Actual	Percent Error
1	1.00	1.00	5.41E-01	1.00	1.00	1.56E-02
2	1.00	1.00	3.18E-01	1.00	1.00	7.89E-03
3	1.00	1.00	-5.58E-01	1.00	1.00	1.17E-03
4	1.00	1.00	-3.33E-01	1.00	1.00	4.07E-03
5	1.00	1.00	-1.13E-01	1.00	1.00	7.85E-04
6	1.00	1.00	3.62E-01	1.00	1.00	2.74E-04
7	1.00	1.00	2.75E-01	1.00	1.00	1.78E-03
8	1.00	1.00	-2.19E-01	1.00	1.00	1.64E-03
9	1.00	1.00	-4.34E-01	1.00	1.00	2.45E-03
10	1.00	1.00	5.43E-02	1.00	1.00	6.62E-04
11	1.00	1.00	6.11E-01	1.00	1.00	2.93E-03
12	1.00	1.00	2.43E-01	1.00	1.00	4.23E-04
13	1.00	1.00	-6.53E-01	1.00	1.00	3.51E-03
14	1.00	1.00	-7.83E-01	1.00	1.00	1.93E-03
15	1.00	1.00	8.59E-01	1.00	1.00	4.94E-03
16	1.00	1.00	3.70E-01	1.00	1.00	3.74E-03

Table A.28 Results for Case 3 for simply supported beam system (continued)

Element Number	$\beta_m = m / m^*$			$\beta_k = k / k^*$		
	Calculated	Actual	Percent Error	Calculated	Actual	Percent Error
17	1.11	1.11	-1.32E-01	1.18	1.18	-9.81E-03
18	1.00	1.00	-7.74E-02	1.00	1.00	2.639E-03
19	1.00	1.00	7.11E-01	1.00	1.00	4.59E-03
20	1.00	1.00	-6.92E-01	1.00	1.00	-1.38E-03
21	1.00	1.00	-5.25E-01	1.00	1.00	-2.87E-03
22	1.00	1.00	2.04E-01	1.00	1.00	2.714E-04
23	1.00	1.00	3.46E-01	1.00	1.00	2.185E-03
24	1.00	1.00	-2.22E-02	1.00	1.00	3.97E-04
25	1.00	1.00	-2.87E-01	1.00	1.00	-1.71E-03
26	1.00	1.00	-6.32E-02	1.00	1.00	-9.08E-04
27	1.00	1.00	1.74E-01	1.00	1.00	1.729E-03
28	1.00	1.00	7.78E-02	1.00	1.00	1.533E-03
29	1.00	1.00	-1.39E-01	1.00	1.00	-2.21E-03
30	1.00	1.00	-2.83E-01	1.00	1.00	-6.3E-03

Table A.29 Results for Case 4 for simply supported beam system

Element Number	$\beta_m = m / m^*$			$\beta_k = k / k^*$		
	Calculated	Actual	Percent Error	Calculated	Actual	Percent Error
1	1.00	1.00	8.20E-02	1.00	1.00	1.71E-03
2	1.00	1.00	3.30E-02	1.00	1.00	4.15E-04
3	1.00	1.00	-3.74E-02	1.00	1.00	-7.80E-04
4	1.00	1.00	-5.72E-02	1.00	1.00	-3.40E-04
5	1.00	1.00	4.52E-02	1.00	1.00	6.38E-04
6	1.00	1.00	1.24E-01	1.00	1.00	7.50E-04
7	1.00	1.00	4.62E-03	1.00	1.00	-2.90E-04
8	1.00	1.00	-1.56E-01	1.00	1.00	-1.10E-03
9	1.00	1.00	-1.15E-01	1.00	1.00	-2.80E-04
10	1.00	1.00	1.79E-01	1.00	1.00	1.35E-03
11	1.00	1.00	3.21E-01	1.00	1.00	1.32E-03
12	1.00	1.00	-4.14E-02	1.00	1.00	-1.10E-03
13	1.00	1.00	-5.33E-01	1.00	1.00	-2.70E-03
14	1.00	1.00	-4.02E-01	1.00	1.00	7.35E-05
15	1.00	1.00	9.56E-01	1.00	1.00	5.29E-05
16	1.00	1.00	-2.95E-02	1.00	1.00	1.73E-05

Table A.29 Results for Case 4 for simply supported beam system (continued)

Element Number	$\beta_m = m / m^*$			$\beta_k = k / k^*$		
	Calculated	Actual	Percent Error	Calculated	Actual	Percent Error
17	1.11	1.11	-1.78E-01	1.18	1.18	-1.1E-02
18	1.00	1.00	1.38E-01	1.00	1.00	4.19E-03
19	1.00	1.00	1.25E00	1.00	1.00	7.41E-03
20	1.00	1.00	-6.22E-01	1.00	1.00	-1.6E-03
21	1.00	1.00	-1.22E00	1.00	1.00	-6.9E-03
22	1.00	1.00	-3.53E-01	1.00	1.00	-1.7E-03
23	1.00	1.00	4.00E-01	1.00	1.00	7.93E-03
24	1.00	1.00	2.39E-02	1.00	1.00	7.56E-03
25	1.05	1.05	8.41E-02	1.21	1.21	-4.9E-03
26	1.00	1.00	-7.2E-01	1.00	1.00	6.5E-03
27	1.25	1.25	1.83E-01	1.22	1.22	1.18E-04
28	1.00	1.00	-1.53E-01	1.00	1.00	6.86E-03
29	1.00	1.00	-6.43E-01	1.00	1.00	-1.7E-04
30	1.00	1.00	-8.53E-01	1.00	1.00	-3.1E-02

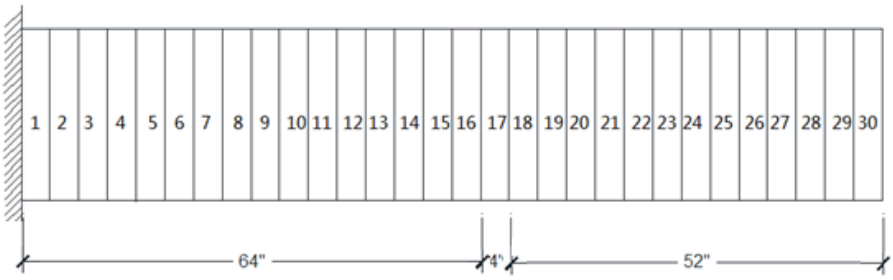

Figure A.1 Cantilever beam model

Table A.30 Damage case description for cantilever beam system

	Case	Location	β_m	α_m	β_k	α_k
Multiple locations	1	3^{rd}	1.25	-0.20	1.14	-0.12
		17^{th}	1.11	-0.10	1.18	-0.15
		25^{th}	1.05	-0.05	1.21	-0.18

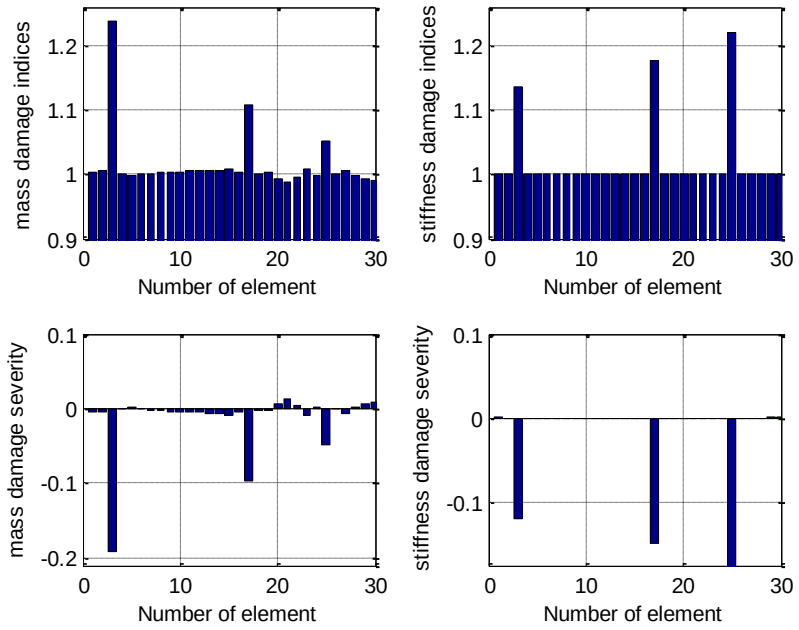

Figure A.2 Calculated damage indicators for Case 1 for cantilever beam

Table A.31 Results for Case 1 for cantilever beam system

Element Number	$\beta_m = m / m^*$			$\beta_k = k / k^*$		
	Calculated	Actual	Percent Error	Calculated	Actual	Percent Error
1	1.00	1.00	3.60E-01	1.00	1.00	-2.40E-02
2	1.00	1.00	4.71E-01	1.00	1.00	-7.30E-03
3	1.00	1.00	-9.47E-01	1.00	1.00	8.45E-03
4	1.00	1.00	-3.98E-02	1.00	1.00	1.09E-02
5	1.00	1.00	-1.90E-01	1.00	1.00	7.77E-03
6	1.00	1.00	2.88E-02	1.00	1.00	3.56E-03
7	1.00	1.00	1.81E-01	1.00	1.00	-1.40E-03
8	1.00	1.00	2.93E-01	1.00	1.00	-6.40E-03
9	1.00	1.00	3.75E-01	1.00	1.00	-1.10E-02
10	1.00	1.00	4.32E-01	1.00	1.00	-1.40E-02
11	1.00	1.00	4.74E-01	1.00	1.00	-1.60E-02
12	1.00	1.00	5.12E-01	1.00	1.00	-1.50E-02
13	1.00	1.00	5.67E-01	1.00	1.00	-1.00E-02
14	1.00	1.00	6.6E-01	1.00	1.00	-1.10E-03
15	1.00	1.00	7.95E-01	1.00	1.00	1.51E-02
16	1.00	1.00	4.60E-01	1.00	1.00	4.24E-02

Table A. 31 Results for Case 1 for cantilever beam system (continued)

Element Number	$\beta_m = m / m^*$			$\beta_k = k / k^*$		
	Calculated	Actual	Percent Error	Calculated	Actual	Percent Error
17	1.11	1.11	-3.58E-01	1.00	1.00	-1.10E-02
18	1.00	1.00	1.38E-01	1.00	1.00	4.19E-03
19	1.00	1.00	2.47E-01	1.00	1.00	7.41E-03
20	1.00	1.00	-6.22E-01	1.00	1.00	-1.60E-03
21	1.00	1.00	-1.22E00	1.00	1.00	-6.90E-03
22	1.00	1.00	-3.53E-01	1.00	1.00	-1.70E-03
23	1.00	1.00	9.00E-01	1.00	1.00	7.93E-03
24	1.00	1.00	-2.76E-01	1.00	1.00	7.56E-03
25	1.00	1.00	8.41E-02	1.00	1.00	-4.90E-03
26	1.00	1.00	-7.20E-03	1.00	1.00	6.50E-03
27	1.00	1.00	6.83E-01	1.00	1.00	1.18E-02
28	1.00	1.00	-1.53E-02	1.00	1.00	6.86E-04
29	1.00	1.00	-6.43E-02	1.00	1.00	-1.70E-02
30	1.00	1.00	-8.53E-02	1.00	1.00	-3.10E-02